

ETH ZÜRICH

MASTER'S THESIS

---

# A Modular Framework for Training Deep Neural Networks on FPGAs using OpenCL

---

*Author:*

Houssam NAOUS

*Supervisor:*

Prof. Dr. Torsten HOEFLER

*Co-Advisors:*

Dr. Tal BEN-NUN

Johannes DE FINE LICHT

*A thesis submitted in fulfillment of the requirements  
for the degree of Masters of Science in Computer Science*

*in the*

Scalable and Parallel Computing Lab  
Computer Science Department

September 1, 2018



Eidgenössische Technische Hochschule Zürich  
Swiss Federal Institute of Technology Zurich

## Declaration of originality

The signed declaration of originality is a component of every semester paper, Bachelor's thesis, Master's thesis and any other degree paper undertaken during the course of studies, including the respective electronic versions.

Lecturers may also require a declaration of originality for other written papers compiled for their courses.

I hereby confirm that I am the sole author of the written work here enclosed and that I have compiled it in my own words. Parts excepted are corrections of form and content by the supervisor.

**Title of work** (in block letters):

A Modular Framework for Training Deep Neural Networks on FPGAs using OpenCL

**Authored by** (in block letters):

*For papers written by groups the names of all authors are required.*

**Name(s):**

Naous

**First name(s):**

Houssam

With my signature I confirm that

- I have committed none of the forms of plagiarism described in the 'Citation etiquette' information sheet.
- I have documented all methods, data and processes truthfully.
- I have not manipulated any data.
- I have mentioned all persons who were significant facilitators of the work.

I am aware that the work may be screened electronically for plagiarism.

**Place, date**

Zürich, 31/08/2018

**Signature(s)**

*For papers written by groups the names of all authors are required. Their signatures collectively guarantee the entire content of the written paper.*

ETH ZÜRICH

# *Abstract*

Computer Science Department

Masters of Science in Computer Science

## **A Modular Framework for Training Deep Neural Networks on FPGAs using OpenCL**

by Houssam NAOUS

Deep Learning has manifested itself into our daily lives. It has become increasingly useful in solving many pattern recognition tasks that were once considered unsolvable in the past. We observe that the trends in deep neural networks are towards deeper and more complex networks. Coupled with the availability of massive datasets, the training time of neural networks increases and becomes harder to accelerate. Recent advancements in Field Programmable Gate Array (FPGA) technologies have sparked interest and thus we see both researchers and application scientists looking into ways of integrating FPGAs into their workflows for utilizing the soft architectures to achieve better performance with low energy consumption. In this work we bridge the gap between research and application and build a framework specifically for translating deep learning models into efficient FPGA binaries using OpenCL. Our framework allows not only to build models, but extends to also verify the functionality of the neural network layers separately, and perform training of the networks on the FPGA itself. We tested the framework with different models and compared the tradeoffs of different approaches while highlighting the challenges of adopting FPGAs for accelerating the next generation of deep neural networks.



# *Acknowledgements*

I would first like to thank Prof. Hoefler of the Computer Science Department at ETH for supporting me and advising me throughout this work. I would also like to thank my co-advisors both Dr.Tal Ben-Nun and Johannes de Fine Licht. I learned a lot from them and they were always available for answering questions. They allowed this paper to be my own work, but steered me in the right the direction whenever I needed it.

I would also like to acknowledge the Swiss National Supercomputing Centre ( CSCS ) for providing us with the hardware and infrastructure necessary for this work and for their prompt response when something went wrong.

Finally, I must express my very profound gratitude to my family and to my friends for providing me with unfailing support and continuous encouragement throughout my years of study and through the process of researching and writing this thesis. This accomplishment would not have been possible without them.

Thank you.

Author

*Houssam Naous*



# Contents

<b>Acknowledgements</b>	<b>v</b>
<b>1 Introduction</b>	<b>1</b>
1.1 Deep Learning and Applications	1
1.1.1 History	1
1.1.2 Learning in Artificial Neural Networks	1
1.1.3 Deep Learning	2
1.2 Modern FPGAs	2
1.2.1 The Case for FPGAs	2
1.2.2 FPGAs vs GPUs	3
1.3 High-Level Synthesis and OpenCL	3
1.3.1 FPGA Workflow	3
1.3.2 High-Level Synthesis	4
1.3.3 Xilinx and Intel	5
1.3.4 OpenCL for FPGAs	5
1.4 Related Work	6
1.5 Motivation	7
1.6 Outline of Next Sections	7
<b>2 Deep Neural Networks and Parallelism</b>	<b>9</b>
2.1 Deep Learning Applications	9
2.2 Convolutional Neural Networks	10
2.2.1 Case Study : LeNet-5	10
Architecture	10
2.2.2 Modern Architectures	12
AlexNet	12
ResNet	13
2.3 Training and Backpropagation	13
Gradient Descent	14
2.4 Parallelism in Deep Neural Networks	16
2.4.1 Data Parallelism	16
2.4.2 Model Parallelism	16
2.4.3 Pipeline Parallelism	17
<b>3 Hardware Implementation</b>	<b>19</b>
3.1 LeNet Pilot	19
3.2 Layer Implementations	19
3.2.1 Convolution Layer	19
Simple Implementation with Unrolling	20
Sliding Buffer Implementation	21

	Row-stationary Implementation . . . . .	23
	Other Implementations . . . . .	24
3.2.2	Maxpool Layer . . . . .	24
3.2.3	Non-Linearities . . . . .	25
3.2.4	Softmax . . . . .	26
3.2.5	Backpropagation . . . . .	26
3.3	OpenCL Kernel Template Generator . . . . .	28
3.4	Integration with Deep500 . . . . .	30
<b>4</b>	<b>Experiments and Results</b>	<b>33</b>
4.1	Convolution Implementations . . . . .	33
4.1.1	Part I : Simple Example . . . . .	33
4.1.2	Part II : Performance in a Real-Case . . . . .	34
4.2	Pipelined vs. Non-Pipelined Inference . . . . .	36
4.3	Training LeNet . . . . .	38
4.3.1	Reconfiguration Time . . . . .	38
	Challenges . . . . .	39
4.3.2	Simple Classifier . . . . .	39
<b>5</b>	<b>Intel OpenCL SDK Primer</b>	<b>41</b>
5.1	Development Workflow . . . . .	41
5.2	Single Work-item vs ND-Range Kernel . . . . .	42
5.3	Inferring Shift-Registers . . . . .	43
5.4	Reconfiguring the FPGA . . . . .	43
5.5	Loops . . . . .	44
5.6	Loop-Carried Memory Dependencies . . . . .	44
5.7	Using Multiple Queues . . . . .	47
<b>6</b>	<b>Conclusion</b>	<b>49</b>
	<b>Bibliography</b>	<b>51</b>



# Chapter 1

## Introduction

### 1.1 Deep Learning and Applications

#### 1.1.1 History

The first artificial neural network traces back to 1958 where it was first conceived by psychologist Frank Rosenblatt [40]. It was called the perceptron and it was meant to model the way a human brain adapts to inputs from the external world to learn binary classification tasks. At some point someone realized that this model could be useful in pattern matching tasks. The artificial neural network is organized into layers of a single threshold logic unit that models a single neuron in the human brain. In the early days, these models were constructed physically and later on were simulated on a single computer [33]. Nowadays, learning tasks are distributed and coordinated on multiple machines to achieve a single learning task [14]. The primitive perceptron developed into a structure of layers organized and separated by non-linearities. In theory, the “Universal Approximation Theorem” states that a multi-layer perceptron with one hidden layer containing a finite number of neurons can approximate any continuous function under some assumptions on the activation function [12].

#### 1.1.2 Learning in Artificial Neural Networks

Towards the end of 1986, Hinton’s paper titled “*Learning representations by back-propagating errors*” [42] was published and it introduced the usefulness of an algorithm called back-propagation. With backpropagation, one can train an artificial neural network composed of multiple layers. It proved more useful than the previously known perceptron-convergence algorithm [52] and by the end of the 1980s many scientific institutes adopted the use of neural networks and utilized them to solve many tasks [38]. Unlike standard algorithms that rely on conditional procedures and hand-crafted logic, the artificial neural network, if designed properly, is robust to noise and can adapt to those pattern matching tasks [51]. Artificial neural networks are exposed to thousands or millions of datapoints that are forward propagated through the weights in each of the layers [30]. In-between each layer non-linearities are introduced and the output is compared to a specific target encoding of the output labels. From that a loss can be calculated and using backpropagation [42], the network readjusts its weights to better match the target output,

specifically reinforcing the connections that contribute to a correct output label.

### 1.1.3 Deep Learning

As computing resources became cheaper and more available and after the numerous improvements in computer hardware and architecture, scientists were able to simulate more complex networks with more neurons and deeper layers [19]. In fact, it was even proven that deeper networks with less neurons per layer proved more useful than the shallow networks [48], thus the concept of deep learning was popularized. Deep learning is only a subset of the broader concept of machine learning which consists of supervised, semi-supervised, and unsupervised learning tasks. It has proven itself useful in applications related to computer vision, speech, recognition, finance, and many others. The hype over deep learning increased even more when these networks were trainable on Graphics Processing Units ( GPUs ) which are capable of performing floating point operations on hundreds and thousands of cores in parallel [39]. This kind of parallelization decreased training time for these networks drastically [39] and soon enough the suitable frameworks were developed and popularized [1, 4]. Researchers were then able to utilize those pieces of hardware for training neural networks with more data and experiment with more sophisticated network models and architectures [23, 39, 19].

## 1.2 Modern FPGAs

### 1.2.1 The Case for FPGAs

The market for Field-Programmable Gate Arrays (or FPGAs) has been increasingly growing and is expected to reach \$12.98 billion by 2023 with a compound annual growth rate of 9.0%<sup>1</sup>. The demand for FPGAs was sparked by the need for high-throughput and low latency applications in industries such as aerospace, finance, and security. FPGAs are integrated circuits that are manufactured in a way such that they can be configured after production [10]. Using hardware descriptive languages ( HDL ) a hardware engineer can build a specific circuit and transfer it to the FPGA where it can reconfigure itself and rewire to implement a given circuit design. They offer a cheaper alternative to high-performing and specialized ASICs as they require less recurring engineering/manufacturing costs and less time to market which is necessary to thrive in this fast-paced economy. They offer a whole new dimension of customization in which complex instruction pipelines can be designed and implemented as opposed to the fixed instruction set architecture of a microcontroller or a generic CPU [28].

---

<sup>1</sup><https://globenewswire.com/news-release/2017/11/29/1210234/0/en/Global-Field-Programmable-Gate-Array-FPGA-Market-to-Reach-USD-12-989-1-million-by-2023.html> Last Accessed : 22/08/2018

### 1.2.2 FPGAs vs GPUs

Application scientists have favored in the last couple of years the use of GPUs to accelerate deep learning tasks [39]. The GPUs architecture lends itself perfectly to perform parallel floating point computations needed to compute and train the networks. Moreover, what has lead to the GPUs more widespread use is a well defined programming model and tool-sets that are easily adopted by software programmers [13]. Dealing with those needs little experience in hardware architecture and applications have been parallelized and scaled massively. FPGAs on the other hand can offer higher power efficiency for the same computational workload as that of a GPU and are intrinsically parallel devices [36]. However it's speed has not yet caught up with it's accelerator counterpart. Power efficiency is a major concern for large-scale applications operating in data centers. For that we have seen most recently both Microsoft<sup>2</sup> and Amazon<sup>3</sup> have incorporated FPGAs into their existing cloud computing infrastructure both for internal use against their data and as a service offered to clients wishing to utilize the power of reconfigurable architectures. Even though FPGAs up to date have only proven to be more power efficient than GPUs [28, 36], simulations and projections done at Intel Corporation predict that the upcoming generation of FPGAs will also compete with GPUs in terms of performance [36]. The projections show that the new Intel Stratix 10 is estimated to achieve 60% higher performance and 2.3 times less power consumption than the Titan X GPU. It is also important to note that the future of deep neural networks (DNNs) have resorted to fixed point computations and lowered precision up to the point of binary values as in Binarized Neural Networks [21]. All of these innovations have lead to irregular types of parallelism in which FPGAs excel at compared to GPUs. GPUs can only operate on a fixed set of data types and thus the trend towards lowering precision tips the scale of performance towards FPGAs [21, 43, 36]. The gap in performance between FPGAs and GPUs is getting smaller and thus it is necessary to update the toolset and design workflows in designing FPGA applications to keep up and make them more accessible for developers to be able to experiment and test.

## 1.3 High-Level Synthesis and OpenCL

### 1.3.1 FPGA Workflow

One of the main reasons that has lead to the slow adoption of FPGAs into commercial applications is the steep learning curve and technical background in hardware design required to be able to design and deploy applications. The usual workflow differs from that of a typical CPU application, however

---

<sup>2</sup><https://www.microsoft.com/en-us/research/blog/microsoft-unveils-project-brainwave/>  
Last Accessed: 22/08/2018

<sup>3</sup><https://aws.amazon.com/ec2/instance-types/f1/> Last Accessed: 22/08/2018

analogies can be drawn to bridge the gap between the two classes of applications. While designing a CPU application starts with a high-level programming language like C++ or Python, designing an FPGA circuit requires the use of hardware descriptive languages. The two most popular hardware descriptive languages are Verilog and VHDL [53]. Some FPGA design tools also offer the designer graphical user interfaces to draw schemas by dragging and dropping boxes. The latter, however, doesn't scale for larger projects and makes it harder to collaborate within a team. HDLs are dataflow programming languages that allow for broader descriptions of how digital circuits can communicate and execute logic in ways where other procedural languages like C fall short. An FPGA application designer also has additional stages in the design cycle where behavioural simulation as well as timing simulations and functional simulations of the design must be performed. After that there is a synthesis, placement, and fitting steps in which the designer hands his design to a piece of software that performs optimizations and tries to materialize the design in terms of a binary file which can be loaded onto the FPGA. Following that the developer runs also more tests on a development board and makes sure to fix any remaining bugs or errors. Another difficulty is that FPGA designs are not portable and thus certain parameters always need to be tuned to adapt to different boards with varying configurations. Each FPGA comes with a different operating specification and different resource blocks<sup>4</sup>, so in order to maximize utilization, the developer is expected to customize their design for each and every board.

### 1.3.2 High-Level Synthesis

High-Level Synthesis (HLS) is not a new invention at all. It has always co-existed with FPGAs. From initial research into HDLs, HLS tools have advanced into C-based dataflow programming paradigms nowadays. We see the level of abstraction rising from gate level, to register-transfer level, into algorithmic level synthesis [17, 32]. HLS is mainly motivated by the need to abstract hardware design to application programmers who should focus on designing and optimizing algorithms regardless of the underlying hardware. This isolation leaves hardware designers with the responsibility of optimizing intermediate representations of algorithms into synchronized logic blocks. Modern HLS tools begin by compiling the input specifications. Many code optimizations like code folding and dead-code elimination are carried-out to get a near-optimal input specification [17]. A control dataflow graph (CDFG) is created that parses the specification into a graph formed of nodes which are the basic blocks and connections that represent control dependencies between those blocks. The results is a register-transfer level (RTL) representation. It consists of a datapath (memory elements, interconnects, and functional units) and a control path (controller). The controller is a finite-state machine that coordinates the flow of elements and operations on the datapath. The RTL representation is then verified to make sure it meets

---

<sup>4</sup><https://www.intel.com/content/www/us/en/fpga/devices.html> Last Accessed 23/08/2018

timing constraints and transformed into a gate-level representation that is then synthesized onto an FPGA according to a board specification file.

### 1.3.3 Xilinx and Intel

We have briefly motivated the main goal of HLS in abstracting the process of hardware design and mapping onto FPGAs. The two main manufacturers and technology leaders in the FPGA market are Xilinx and Intel (after the acquisition of Altera in 2015). Both companies have shifted their tool-sets to favor higher-level abstractions for synthesis but they have taken slightly different approaches. We note that Xilinx’s development workflow favors more the hardware engineer by giving more control for them to view/modify designs and control most of the nuts and bolts that transform their applications into hardware [54]. Altera’s tools however favor the software developer wishing to leverage hardware accelerators to achieve higher throughput for their application. The Intel FPGA developer is provided with a programming manual that suggests code improvement so that a better hardware design is generated. Both companies have adopted the use of HLS tools that can transform code in behavioural C/C++ and OpenCL descriptions into bitstreams [54, 24].

### 1.3.4 OpenCL for FPGAs

OpenCL™ ( Open Computing Language ) is the open standard for cross-platform parallel programming that is a subset of the C standard [46]. OpenCL provides a programming model that fits the GPU architecture perfectly and is able to exploit parallelism through vectorized operations. GPUs are able to perform vectorized operations and have higher memory bandwidth than CPUs, enabling them to achieve high throughput by doing parallel floating point operations. We mentioned in section 1.3.3 that OpenCL has also been adopted for high level synthesis on FPGAs. The challenge in adopting OpenCL for FPGAs is being able to not only vectorize operations but to also create efficient pipelines that fully utilize the resources available on the board. For that the Intel OpenCL SDK [24, 28] performs those optimizations and allows the user to use pre-defined pragmas in order to adapt OpenCL code for FPGAs. This again beats the goal for portability across platforms when different customizations have to be introduced for FPGAs, however pipeline parallelism and complex data-flow instructions prove to be an advantage and a necessary feature that should be exploited on FPGAs [3, 28]. It is also worth noting that effort for optimizing the same OpenCL kernel differs between FPGAs and GPUs, putting FPGAs at a slight disadvantage. The reason is that with GPUs, the developer looks for the best mapping into the fixed architecture, while for FPGAs the developer guides the compiler into finding the best control and memory architecture for the given task. Moreover, compiling OpenCL kernels for FPGAs takes much longer than on GPUs as more board-specific optimizations can be done and because FPGAs allow for a broad design-exploration space.

## 1.4 Related Work

An implementation called “PipeCNN” [50] using OpenCL has explored the power of pipelining neural network layers to lower the overall memory bandwidth requirement in between network layers. The implementation was able to achieve a maximum throughput of 12.8GB/s on the Altera Stratix-5 board. The implementation however only covers convolution layers and fully connected layers. A single matrix-multiplication based kernels implements both of the convolution and fully connected layers and pipelines them with a pooling operation. In this implementation, full inter-layer communication is done by communicating through global memory. Local response normalization (LRN) which is done after the pooling layer is not pipelined directly and also communicated through global memory. The implementation, even though it utilizes the full memory bandwidth of the board, requires a lot of overhead for inter-layer communication and can be further reduced by pipelining more layers together.

The work of DiCecco et. al [15] utilizes the Xilinx SDAccel<sup>5</sup> toolset for optimizing neural network designs. They implement an FPGA backend for the popular neural network framework Caffe [26]. This methodology makes use of the already existing testbenches in Caffe for verifying correctness of the FPGA implementations. The authors run experiments using modern deep neural nets such as Alexnet[27], GoogleNet [48], and VGG-16[44] and achieve a maximum throughput of 50 GFLOPS across the 3x3 convolutions on the Xilinx Virtex 7. The authors also implement convolution using the Winograd [29] minimum filtering algorithm. This filtering scheme minimizes the number of multiplications required due to overlapping intermediate results in overlapping filter computations. The work lays the stepping stones and mentions the challenges in integrating FPGAs as accelerators for popular DNN frameworks like Caffe such as long reprogrammability times ( 100-400ms for FPGA vs 0.001ms-0.005ms for a GPU ) and thus different types of parallelism should be exploited to fill in the gaps. FPGA implementations also require offline compilation and several vendor specific attributes to achieve optimal performance. The results are not impressive showing that GPU performance is still higher and the framework is still far from integrating the different layers of a DNN other than convolutions.

Zhang et. al.[55] were able to achieve 61.2 GFLOPS under 100 MHz on a VC707 FPGA. The main contribution of this work is an analysis framework which takes into consideration both the computing resources and the memory bandwidth provided by the board to guide the design space exploration phase. They balance out loop unrolling factors and loop tiling methods to balance the tradeoffs of using compute resources and memory bandwidth. The work however only focuses on the inference phase and lacks the analysis of the training phase of a CNN which could take days or weeks for a single learning task. They also focus on single layer optimizations for and not on multiple layer optimizations. This is important as compute intensive

<sup>5</sup>/url<https://www.xilinx.com/products/design-tools/software-zone/sdaccel.html> Last Accessed: 23/08/2018



layers like convolutions can be balanced out with bandwidth hungry layers like the fully connected layers to achieve better performance.

## 1.5 Motivation

This work aims to leverage the benefits of OpenCL for programming FPGAs and target implementations of modern deep neural networks. The field has gained a lot of traction and so far the support for FPGA backends for accelerating neural network computations are still research based and experimental. It is also becoming increasingly important to utilize FPGA's configurable circuits for latency-sensitive and real-time DNN applications such as autonomous driving. By using FPGAs, neural networks can be accelerated and energy efficient by utilizing pipeline parallelism [3, 28]. Besides from that, an additional goal is not only to create networks for inference but to also accelerate training of deep neural networks on FPGAs. For that we use the Lenet network as a case study and proof of concept and implement mini-batch gradient descent for training this network. We also aim to bridge the gap between research and application, so we have created a framework in Python that is able to go from open source model definitions like ONNX [37] into material FPGA implementations. The development framework is easily extensible with modular components that also allow for individual customization and research into novel ways of accelerating the layer computations, backpropagation, and full network pipelining as a whole.

## 1.6 Outline of Next Sections

- Chapter 2 explains the algorithms and terminology in deep learning.
- Chapter 3 explains the toolset and hardware implementation of deep neural networks on FPGAs.
- Chapter 4 analyzes and discusses the results of the experiments of running the implementation on the FPGA.
- Chapter 5 serves as a primer and best practices in using OpenCL for FPGAs.
- Chapter 6 contains the concluding remarks and future direction of work.





## Chapter 2

# Deep Neural Networks and Parallelism

## 2.1 Deep Learning Applications

Deep learning and the progress made in that field have all fueled its integration into many applications of daily life [3]. In the early days, the results of machine learning were dependent on the quality and informativeness of the features fed into the learning algorithm [12]. With the development of deep neural nets, the machine itself can abstract raw data and learn complex features that become much more informative than the hand-engineered ones [30]. Modern architectures are able to process and incoming stream of images, video, or speech and learn to classify those raw data and solve complex problems in image segmentation and speech recognition [30, 19, 23]. What is also important is that the value gained by those architectures increases as more data and more computational resources are presented to the network for training. Learning can be supervised, semi-supervised, and unsupervised [30]. Supervised learning is a problem of finding the best mapping between a set of input data  $X$  and a set of output labels or values  $Y$  [30]. Learning algorithms proceed in approximating the mapping function  $f : X \rightarrow Y$  by observing both the inputs and the labels. Learning stops when an acceptable approximation of  $f$  is found. Supervised learning can be split into two categories; classification when the output variable is a given label as in objects : *"table"* , *"penguin"* , or *"motorcycle"*, and regression when the output variable is a real-value such as *"temperature"* or *"dollar value"*. The goal of unsupervised learning on the other hand is to discover a data model or structure of the given data. There are no given labels or output variables and the goals is to learn something useful about the data. Unsupervised learning is split also into two categories; clustering by splitting the data into groups having similar attributes, and association where we want to discover rules that describe a large subset of the observed data ( ex. People who work at *"X"* tend to buy product *"Y"* ). Semi-supervised learning is situated somewhere in between supervised and unsupervised learning where only a subset of the data is labeled. Solving these problems requires both supervised techniques to label the unlabeled data and feed back in the labels for training, or the data can be used to uncover structure. Our work focuses more on supervised learning as the majority of deployed applications use supervised learning. We attempt

to accelerate the training process of deep neural networks on FPGAs.

## 2.2 Convolutional Neural Networks

Convolutional Neural Networks have achieved many successes in multidimensional data than can be represented as arrays [31, 27, 19]. A typical image can be represented as a three-channeled ( Red, Green, and Blue ) two-dimensional array of varying pixel intensities. A convolutional neural net is mainly composed of two stages that make sense of structured grid-like data to accomplish a learning task such as classification, regression, or even dimensionality reduction. An initial stage of convolution operators that pass a window filter over the image to extract an output feature map as in a discrete convolution operator. The convolution operation was inspired by a cat's visual cortex and how neurons in the brain are triggered by certain shapes like lines in the seen image [22]. The intuition behind the convolution operation as a feature extraction method is that nearby pixels exhibit similarities and show high correlations [29]. Also the image patches extracted in the convolution windows which represent concepts can appear anywhere elsewhere in the image. The convolution layers are usually followed by non-linear activations and then pooling operators. The role of pooling layers is to merge the similar nearby features into one to decrease the sensitivity of the network to the position of the extracted feature [48]. The second stage of a CNN is a series of fully connected layers ultimately terminating at an output layer.

### 2.2.1 Case Study : LeNet-5

The LeNet [31] model is considered to be the first demonstration of a convolutional neural network and was proposed by LeCun et. al [31] in 1998. Its architecture has shown record accuracy in classifying digits and was deployed commercially for identifying characters on personal and business checks. LeCun's work was the first to demonstrate the benefit of brute-force numerical tricks in convolutions and that these tricks can be more useful than hand-engineering traditional feature engineering techniques [31]. Also compared to traditional neural networks, the convolution layers are more robust as the extracted features are shift and translation invariant. This proved to be efficient since handwritten characters differ in slant and scale from one person's handwriting to another's and it was hard back then to perform feature pre-processing to documents such as normalization and centering handwritten characters.

#### Architecture

The Lenet-5 is comprised of 7 layers ( excluding the input layer ), all of which contain trainable parameters. The input is a centered 32x32 image which represents the raw data that is fed into the network. It is followed by a convolutional layer and a subsampling layer. The first convolutional layer C1 produces an output of 6 distinct feature maps. Each feature map is obtained

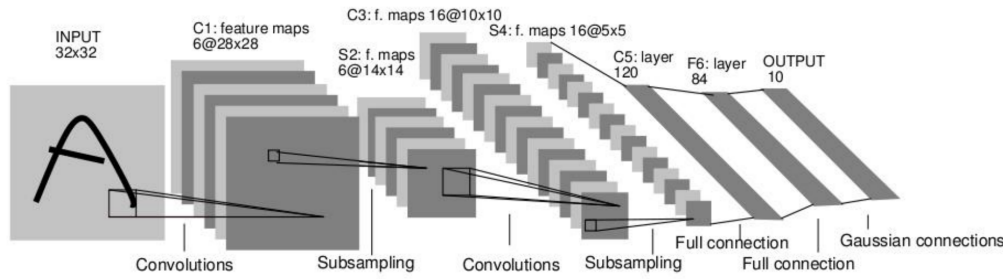


FIGURE 2.1: LeNet-5 Architecture, a convolutional neural network used for character recognition. [31]

by sliding a  $5 \times 5$  filter along the input image and computing a weighted sum of the pixels inside the window. This leads to shrinking the image by 4 pixels along both dimensions, and 6 features are obtained by passing 6 different weights for the filters. A bias is added to the weighted sum of pixels and it is squashed by the sigmoid function before feeding into the output feature map.

The convolutional layer is then followed by a subsampling layer with a window size of  $2 \times 2$ . The four feature maps elements in C1 are added, multiplied by a trainable coefficient and then a trainable bias is added. The six feature maps of C1 are halved in size along both dimensions and the resulting feature maps at S2 are six  $14 \times 14$  arrays.

	0	1	2	3	4	5	6	7	8	9	10	11	12	13	14	15
0	X				X	X	X			X	X	X	X		X	X
1	X	X				X	X	X			X	X	X	X		X
2	X	X	X				X	X	X			X		X	X	X
3		X	X	X			X	X	X	X			X		X	X
4			X	X	X			X	X	X	X		X	X		X
5				X	X	X			X	X	X	X		X	X	X

FIGURE 2.2: Each column indicates which feature maps in S2 are combined by the units in a particular feature map of C3. [31]

Similarly the feature maps at S2 are followed by another convolution and another subsampling layer C3 and S4. The outputs of S2 however are not connected all-to-all to the third convolution instead only the marked slots in the table 1 below shows that only some combinations of the feature maps in S2 are connected to C3. The purpose is to avoid overfitting to the full S2 features by breaking the symmetry and hopefully discovering different feature abstractions from the different set of inputs [31]. It also serves to decrease the amount of trainable parameters in the model.

The convolution stage ( C1  $\rightarrow$  S4 ) is followed by two fully connected layers C5 and F6 of sizes 120 and 84 neurons respectively. Note that the reason C5 is labeled as a convolution layer (even though it performs the role

of a fully connected layer) is that if the network were scaled for bigger inputs, the output feature map for C5 would be larger than  $1 \times 1$ .

The last fully connected layer is fed into the output which is composed of Euclidean Radial Basis (RBF) [5]. It computes the euclidean distance between the input vector and a trainable parameter vector. The model was trained on a set of 60,000 images and achieved a minimum test-error of 0.7% competing with all of the other neural network models at the time. Some of the input training images were translated slightly, and rotated by up to  $\pm 30^\circ$  to increase the network's robustness by making it slightly more translation and rotation invariant.

Even though the Lenet is outdated and has been replaced by many other neural networks, we choose to this network as a prototype to build our DNN framework due to the simplicity of the implementation. We implement it not for its usefulness but rather more to guide our study into optimizing layer implementations and thinking about methods to improve throughput and achieve pipelining between the layers.

## 2.2.2 Modern Architectures

### AlexNet

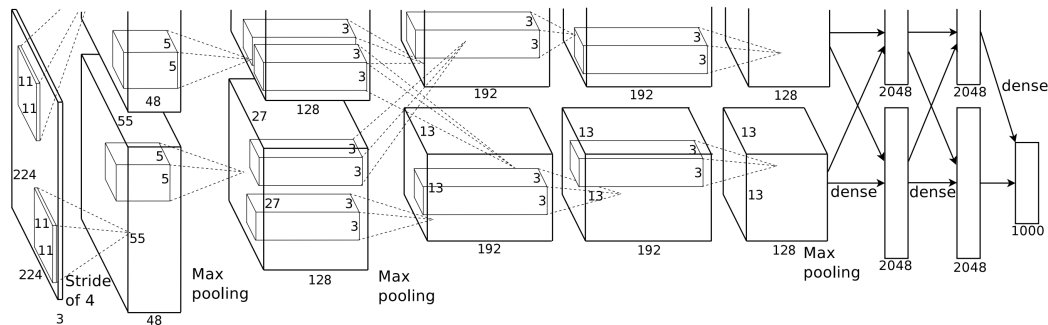


FIGURE 2.3: Alexnet Architecture [27]

The AlexNet [27] model designers won the ImageNet Large-scale Image recognition competition in 2012. It follows LeNet's approach of staging some convolutional layers back-to-back and then eventually terminating with fully connected layers to perform the classification. It was able to achieve 26.25 top-5 error in the task of classification of three-channeled 224x224 images into 1000 classes. The network was trained on a GPU [27] and used local response normalization layers. In addition to that the authors used dropout which is a technique against overfitting in a network [45]. It involves randomly picking out neuron connections and setting them to zero thus decreasing the number of trainable parameters in the model. What also differs from LeNet is the use of Rectified Linear Units (ReLU) activations and maxpooling [27] for the subsampling layers.

## ResNet

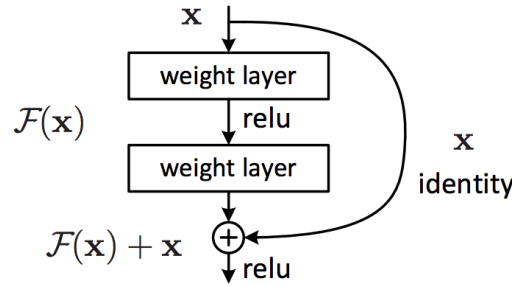


FIGURE 2.4: A basic building block in residual networks showing the identity shortcut [19]

ResNet [19] is one of the modern networks that sacrifices breadth for depth. Training deeper network is harder because of a problem discovered by Hochreiter et al. [20] of vanishing gradients. The authors of ResNet augment the network with shortcut connections that act as identity layers and enable training with respect to residuals instead of the original input values. Using this trick it was possible to train deeper networks reaching up to more than 150 layers [19].

## 2.3 Training and Backpropagation

The above networks all try to achieve the goal of properly approximating a mapping function between the dataset inputs and the given labels. In the example of Lenet, inputs are normalized 28x28 single channels, and the output of the network is a the most probable digit between 0 and 9 that this image represents. Formally described, given an input domain  $X$ , an output set of labels  $Y$ , and a set of candidate functions  $f : X \rightarrow Y$  belonging to a hypothesis class  $H$ , we are trying to minimize the loss of mispredicting the correct class. The loss function can be expressed as :

$$L_D(f) = p(f(z) \neq h(z)) \quad (2.1)$$

where  $z$  is a sample from the dataset  $D$ ,  $f(z)$  is the output prediction and  $h(z)$  is the true class or label. In that case training is then formalized as finding the best set of parameters  $w$  in our model to minimize this loss function.

$$w^* = \arg \min_{w \in H} L_D(f_w) \quad (2.2)$$

Several options exists for sample loss functions as shown in Table 2.1. In regression, a common loss function is the squared error loss. In classification problems, the binary loss can be used. However, for minimization, the loss function should be both continuous and differentiable. To solve this problem, an alternative cross-entropy loss function is introduced for multi-class classification problems as opposed to the binary loss. The output becomes

a probability distribution of the input according to the given possible output classes. The cross entropy loss calculates the difference between the predicted distribution and the true distribution into  $K$  classes.

Squared loss	$l = (f_w(z) - h(z))^2$
Binary loss	$l = \begin{cases} 0, & \text{if } f_w(z) = h(z) \\ 1, & \text{if } f_w(z) \neq h(z) \end{cases}$
Cross-entropy loss (K classes)	$l = \sum_{i=1}^K f_w(z_i) \log(h(z_i))$

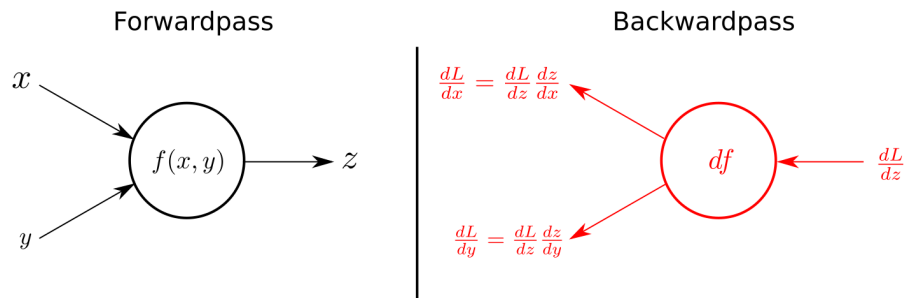
TABLE 2.1: Examples of loss functions

### Gradient Descent

To solve the minimization problem, we can either use evolutionary algorithms [16] inspired by natural processes and meta-heuristics or we can resort to the use of iterative approaches. It is more popular in machine learning to use the iterative gradient descent techniques. In gradient descent, starting from an initial set of weights, we calculate the gradient of the loss function with respect to the weights  $\frac{\partial L}{\partial w}$  and iteratively adjust the weights in the direction of the gradient to minimize loss.

$$w^t = w^{t-1} + \eta \frac{\partial L}{\partial w} \quad (2.3)$$

The error is back-propagated layer by layer from the output to the input layer by utilizing the chain-rule.  $\eta$  is the learning rate, which is a tunable hyperparameter for weight updates.

FIGURE 2.5: Local Gradient Backpropagation using the Chain Rule. Source:<sup>1</sup>

Gradient descent implementations vary depending on how many samples are used to calculate the error. The three main types are batch, stochastic,

<sup>1</sup><https://kratzert.github.io/2016/02/12/understanding-the-gradient-flow-through-the-batch-normalization.html> Last Accessed: 23/08/2018

and mini-batch gradient descent [41]. The different types also exhibit trade-offs in terms of computations required, frequency of updates, convergence, and stability of the calculated gradient.

---

**Algorithm 1: Batch Gradient Descent**


---

```

N = number of training points;
while not converged do
    |  $w^t = w^{t-1} + \eta \sum_{i=0}^N \frac{\partial L}{\partial x_i} \frac{\partial x_i}{\partial w}$  ;
end

```

---

In Batch Gradient Descent (BGD), the error is calculated for all of the samples in the training set. After all of the samples have been observed, the error can be backward propagated through the layers and the weights are updated. This complete forward pass and the backward update is called an epoch and usually neural networks are given a fixed set of epochs to train or we keep training until a certain accuracy is achieved. The benefit of using batch gradient descent is that the complete gradient is computationally efficient and presents stable convergence [41]. Stability on the other hand makes it harder to avoid local minima and the minimization problem can easily get stuck in a local minimum. Knowing that the optimization problem of neural networks is riddled with saddle points, one can resort to different types of gradient descent.

---

**Algorithm 2: Stochastic Gradient Descent**


---

```

N = number of training points;
Randomly Shuffle Data Points;
for  $i=1, \dots, N$  do
    |  $z \leftarrow x_i$  ;
    |  $w^t = w^{t-1} + \eta \frac{\partial L}{\partial z} \frac{\partial z}{\partial w}$  ;
end

```

---

Stochastic gradient descent (SGD) offers an alternative to calculating the full gradient and passing in the whole dataset. Instead, a random sample is selected from the dataset and forward propagated, the weights are then updated after backpropagating the gradient resulting from this sample. This update technique is less stable than batch gradient descent but it helps in avoiding local minima. It has also been proven that it converges with a rate of  $\frac{1}{\sqrt{T}}$  where  $t$  is the iteration number or epoch for convex functions. SGD demands more computational power due to the frequent updates especially when the training set is large.

---

**Algorithm 3: Mini-batch Gradient Descent**


---

```

N = number of training points;
B = batch size;
for  $i=1, 1+B, \dots, N-B+1$  do
    |  $w^t = w^{t-1} + \eta \sum_{j=i}^{j=i+B-1} \frac{\partial L}{\partial x_j} \frac{\partial x_j}{\partial w}$  ;
end

```

---

Minibatch gradient descent comes as the middle ground between SGD



and BGD and is commonly used in practice. The weight update is viewed only after a mini-batch is forward propagated. Typical batch sizes are 32, 64, 128 (sometimes much larger in the thousands) as powers of 2 fit the memory requirements of GPU accelerators and memory specifications. This technique balances the robustness of SGD and the stability of BGD. Minibatch introduces another hyperparameter that increases design space and allows for trying out different values to obtain the best test-accuracy.

## 2.4 Parallelism in Deep Neural Networks

As the models grow in size and have more trainable parameters, more data and computational resources are required to properly train the above networks. For that we can speed up the training process of DNNs by exploiting parallelism from different perspectives. We can distinguish three main types of parallelism [3]; data parallelism by parallelizing over the input dimension, model parallelism by tiling computations and running the same layer concurrently on separate cores, and pipeline parallelism which exploits the pipeline structure of the networks and runs the layers concurrently where one layer's output feeds into the other layer's directly.

### 2.4.1 Data Parallelism

The structure of the input and intermediate results of convolutional neural networks as multidimensional grids allows us to use this structure and split up the input into several parts that can also be forward propagated concurrently. The training samples in a batch gradient descent algorithm can be calculated separately before the back-propagation step. The bottleneck in this approach appears when we wish to back-propagate the error and all of the errors are averaged to calculate the gradient with respect to the loss function. The paradigm is suitable for a MapReduce model and can easily be parallelized. The only obstacle to this approach is batch normalization layers where synchronization has to occur at every normalization layer.

### 2.4.2 Model Parallelism

In this type of parallelism, the neurons in a hidden layer are divided and computed separately. This can decrease the memory requirement for running the network if the model is partitioned but it also adds the overhead of communication between the different parts of the model. For example in an all-to-all connection in fully connected layers, the intermediate results should be shuffled across different computing nodes and synchronized so that the next layer can be computed. Some improvements have been proposed such as adding redundant computations in fully connected layers so that less communication is required[34], but it comes at the expense of more computations. As for convolutional layers, splitting the task of calculating output feature maps across separate processes would induce an overhead of



reading the input map of the previous layer multiple times and is thus impractical [28].

### 2.4.3 Pipeline Parallelism

This type of parallelism is similar in a sense to both of data and model parallelism. The multiple stages of computations and layers in a DNN can be all active at the same time in a pipeline order. The idea is that different stages can be working on different parts of the pipeline as data is ready from an earlier stage. This is specifically important to the rest of the work as this is a type of parallelism that only FPGA accelerators can benefit from. On such flexible architectures, complex dataflows and pipelines can be programmed. Some implementations have shown that forward propagation and the backward pass computations can be pipelined together [2, 9]. The challenge in this is that as deep neural networks become bigger, they may not fit within a standard FPGA resources. Two solutions can thus be proposed. On one hand, the layers can be combined together and the network can perform the computations, reprogram itself and then compute another combination of layers. Communication in that case can be done by reading and writing intermediate results to global memory. Another solution can be implemented using the OpenCL SDK for Xilinx (Intel has not yet added support for that in high level synthesis) leveraging the power of partially reconfiguring an FPGA while part of it is performing computations.



## Chapter 3

# Hardware Implementation

### 3.1 LeNet Pilot

The main contribution in this work is in the form of a framework for the development and optimization of deep neural network operators on an FPGA. We use the LeNet [31] model, knowing that it is outdated and outperformed by many other network architectures discussed before, due to its simplicity and as a pilot to test our framework. The simple network allows us to implement four different types of layers (convolution, maxpooling, fully connected layers, and softmax). We also implement the backward propagation operators for all of the above layers. We use LeNet to guide the numerous optimizations we perform on each layers separately and on the combination of the layers into a pipeline as well. We implement a modern variant of LeNet which only differs slightly from the original one. The first convolution in our model contains 10 feature maps as opposed to 6 in the original lenet2.1, the second convolution outputs 20 feature maps as opposed to 15 feature maps. This adds more trainable parameters and thus we hope to use most of the MNIST dataset for training. For the sub-sampling layers we replace the average pooling operation by the maxpooling operation. We also use ReLU activation functions as opposed to the sigmoid as it has a lighter hardware implementation and it has shown better results than the sigmoid in practice [27]. In the following sections we go more in detail about the implementation of the operators using OpenCL.

### 3.2 Layer Implementations

#### 3.2.1 Convolution Layer

The fundamental operation in Convolutional Neural Networks is the convolution operation. This layer takes as input a multidimensional grid and extracts output feature maps by sliding a window of weights. The filter weights and biases are trainable by gradient descent. An output feature map pixel  $y_i$  is obtained by passing a filter of size  $K_h \times K_w$  over an input feature  $x_i$  with  $CH_{in}$  input channels.

$$y_i = \text{relu} \left( \sum_{c=0}^{c=CH_{in}} \sum_{h=0}^{h=K_H} \sum_{w=0}^{K_w} w_{i,c,h,w} * x_{c,h,w} + \text{bias}_i \right) \quad (3.1)$$

Layer	No. Parameters
C1	260
C2	5,020
C5	117,720
F6	10,164
<b>Total</b>	133,164

TABLE 3.1: Number of Trainable Parameters for Custom LeNet Implementation

The nested loop structure lends itself easily for parallelization. We will discuss three different implementations for this layer and compare tradeoffs that can be used by the user

### Simple Implementation with Unrolling

With the help of high level synthesis, we can write a C-like implementation and analyze the performance. Assuming the kernel is pipelined we will require  $batchsize * Img_h * Img_w * K_h * K_w * CH_{in} * CH_{out}$  cycles theoretically to complete the convolution. To speed up the naive implementation we perform some optimizations:

- **Unroll over filter computation:** Calculating each pixel in the output feature maps requires  $K_h * K_w * CH_{in}$  multiplications. As our filter sizes are small, we can unroll over the filter dimensions. By unrolling we are effectively parallelizing the algorithm by  $25x$  ( since in our case  $K_h = 5, K_w = 5$  ) . However, we choose to unroll over the input channels and the width of the kernel only. We choose input channels as opposed to only the kernel dimensions due to our memory layout because we stripe the input and output feature maps by channels as the lowest rank dimension. This increases memory performance by performing batch aligned memory reads.
- **Buffer the coefficients:** During the forward pass, the filter coefficients, will be read multiple times. For that, we can reduce the amount of memory reads and buffer the coefficients in low-power and fast registers. This uses space on the board but allows us to access coefficients for a relatively cheaper cost.

Summations inside loops, such as in 3.1 can introduce memory dependencies as the result of the next iteration depends on a previous one. Memory dependencies get worse with unrolling factors as the critical path is increased. We carefully transfer the memory dependencies to local memory

on the FPGA (discussed in more detail in 5.6 ) and achieve an ideal iteration index (ii) = 1. Therefore, the theoretical number of cycles for a convolution is expressed as

$$\text{Latency}(L) \approx ii * \text{batchsize} * \text{Img}_h * \text{Img}_w * \text{CH}_{out} * K_h \text{ cycles} \quad (3.2)$$

```

1 #pragma ii 1
2 for(int b = 0 ; b < batch_size ; b++){//loop batch size
3   for(int i =0 ; i < IMAGE_HEIGHT ; i++){ //img height
4     for(int j = 0 ; j < IMAGE_WIDTH ; j++ ){ //img width
5       for(int chout = 0 ; chout < CH_OUT ; chout++){ //output channels
6         float val[WIDTH*HEIGHT*CH_IN]; //local storage of intermediate
          results
7         for(int k = -PAD_H; k <= PAD_H ; k++ ){ //kernel height
8           #pragma unroll
9           for(int l = -PAD_W ; l <= PAD_W ; l++){ //kernel width
10            #pragma unroll
11            for(int z = 0 ; z < CH_IN ; z++ ){ //input channels
12              //Check if out of bounds
13              if( i+k>=0 && i+k<IMAGE_HEIGHT && j+l>=0 && j+l<IMAGE_WIDTH){
14                val[z][k+PAD_H][l+PAD_W] =
15                coeff[chout][k+PAD_H][l+PAD_W][z]*input[b][i+k][j+l][z];
16              } else {
17                val[z][k+PAD_H][l+PAD_W] = 0.0;
18              }
19            }
20          }
21        }
22        float final_val = 0.0;
23
24        #pragma unroll
25        for(int i =0; i < CH_IN*WIDTH*HEIGHT ; i++){
26          //Aggregate partial sums <- reduction
27          final_val += val[i];
28        }
29
30        final_val += bias_buff[chout];
31        //Write Output
32        output[b][i][j][chout] = relu(final_val);
33      } //end chout loop
34    }
35  }
36 }
37 }

```

LISTING 3.1: code snippet from simple convolution

### Sliding Buffer Implementation

In the simple implementation, we buffered the coefficients in low-cost local registers to avoid having to read the coefficients multiple times from memory. We also notice that when the convolution window slides with a stride of 1 step, there will be also values in the input feature map that are re-used. For that, we implement a sliding window that contain's all previously seen

values as long as they can still be useful. Our implementation is similar to what is describe by Zohouri et. al [56]. The shift-register holds the input values and multiple taps allow for accessing the desired values in the sliding window. The intel offline compiler performs optimizations like replicating RAM blocks to allow for simulataneous access. For that, only few compiler directives should be specified to make this implementation work 5.3. This implementations is also an example of how we can trade local storage to minimize bandwidth. We also carry over the optimization done in the simple implementation.

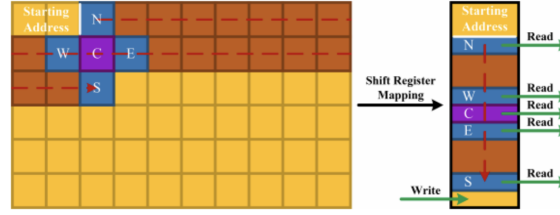


FIGURE 3.1: Sliding Buffer Visualization. Source: [56]

Private Variable: - 'window' (filter.ct:27)	1281	6122	8	0	<ul style="list-style-type: none"> <li>Type: Shift...</li> <li>1 register...</li> <li>63 register...</li> </ul>
Private Variable: - 'x' (filter.ct:22)	24	101	0	0	<ul style="list-style-type: none"> <li>Type: Regi...</li> <li>1 register...</li> </ul>
Private Variable: - 'y' (filter.ct:22)	24	101	0	0	<ul style="list-style-type: none"> <li>Type: Regi...</li> <li>1 register...</li> </ul>
Details					
<b>Private Variable:</b> - 'window' (filter.ct:27): <ul style="list-style-type: none"> <li>Type: Shift Register (72 or fewer tap points)</li> <li>1 register of width 9 and depth 1</li> <li>63 registers of width 32 and depth 1</li> <li>8 registers of width 32 and depth 248</li> </ul>					

FIGURE 3.2: Sliding 'window' variable is inferred as a shift-register by the OpenCL compiler

This implementation proves useful if data is provided in a streamlined fashion. The sliding buffer reads data sequentially and is more suitable for non-blocking dataflow computations.

### Limitations

One of the limitations this implementation is that we quickly run out of buffer space as the dimensions of the problem grow larger. The sliding buffer size grows linearly with the above parameters:  $CH_{in}, Img_w, K_h, K_w$ . For our application in a network as small as the Lenet, we do not worry about this problem. The solution to scaling the sliding buffer implementation is to utilize spatial blocking and tile the input into blocks and perform the computations in these tiles separately such as in [56].

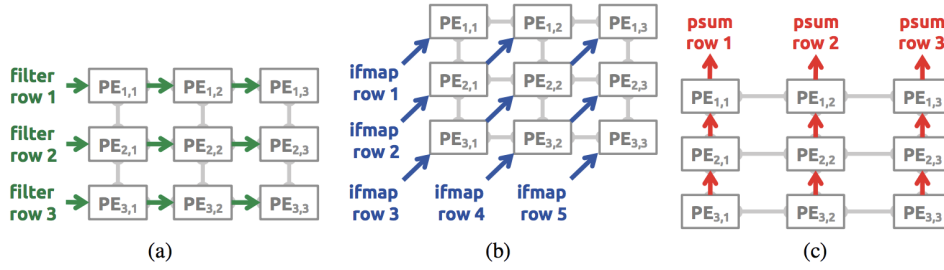


FIGURE 3.3: Datar re-use across processing elements in Eyeriss.

Source: [6]

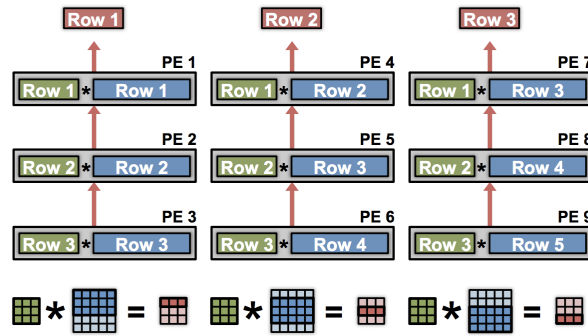


FIGURE 3.4: 2D spatial convolution with a grid of processing elements (Eyeriss). Source: [47]

### Row-stationary Implementation

This approach was suggested by Chen. et. al [6] and it presents a way of reusing both filter weights and input feature maps. The technique requires a set of replicated processing unit. In the simple case of 3x3 filters we can instantiate 9 processing elements (PEs) each holding one of the 3x3 filter weights 3.3. We implemented a simplified version of this architecture using the Intel SDK's autorun kernels, which means the kernels do not need to be explicitly invoked and can communicate data to each other using channels (FIFOs). Input feature maps are then streamed diagonally (blue 3.3) where they are required for the computation of different output feature map rows. The partial sums are accumulated upwards vertically (shown in red 3.3).

The advantages in using this is that the size of this grid can be adjusted to best fit the resources available on a specific board. This dataflow performs the theoretical minimum of memory reads required as input feature maps are read once and communicated diagonally to other PUs based on demand. Communication between PEs is done through Intel OpenCL channels which are Intel's implementation of FIFOs (or pipes in OpenCL terms) and computations are performed asynchronously. Two separate reader and writer kernels handle reading and writing data between global memory and the

processing grid. The size of this grid is reconfigurable and the user can instantiate a larger version of this grid. It is independent of the image and filter sizes as we reuse techniques from Eyeriss [6] such as folding and replication to map different computations onto the same fixed grid.

### Other Implementations

The below methods were **not implemented** but it is worth discussing other approaches to performing a convolution. The shared idea is to transform the convolution operation into another form of computation with different properties thus allowing to perform different types of optimizations.

**Matrix Multiplication:** One solution to the convolution problem involves transforming the input matrix and incorporating redundant data as in [7]. This transforms the convolution operation into a direct matrix multiplication. The downside of using this is the requirement of either a larger storage for storing the redundant inputs or a very complicated memory access pattern to be implemented [3].

**Fast-Fourier Transform (FFT):** Another solution is found by transitioning into the Fourier domain and applying a fourier transform on both the filter and the input image [49]. In the Fourier domain, a convolution becomes again a matrix multiplication. After multiplication of the frequency domain representations of the filter and the input, we use the inverse-fourier transform to obtain the output image. The fourier-transform decreases the complexity of the convolution operation from  $O(N_o^2 N_f^2)$  to  $O(N_o^2 \log_2(N_o))$  where the input image size is  $N_o \times N_o$  and the filter size is  $N_f \times N_f$  [47]. The tradeoff in this case is less operations on the expense of additional bandwidth and storage requirements. The quality of this transformation and benefits degrade for smaller filters and thus fourier is usually used in the case when large input features and filters are required [47].

**Strassen's Algorithm**[11]: can reduce the number of multiplications from  $O(N^3)$  to  $O(N^{2.8})$  [47]. The reduced multiplications lower the space requirement as floating point operators require more space than additions but comes at the expense of numerical stability and storage space requirement to hold and propagate intermediate results [47].

### 3.2.2 Maxpool Layer

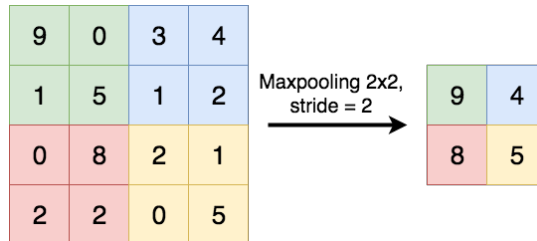


FIGURE 3.5: Maxpooling Operation



Convolution layers are usually followed by subsampling layers such as average pooling and maxpooling [31]. These operations play a main role in decreasing the size of feature maps in the network and also add to the robustness and also make the network slightly shift-invariant and robust against distortions in the image [27]. Two common subsampling operations are the average pooling where the input values within a certain window are averaged and passed as one output feature map. The second type, which we choose to implement is the maxpooling which passes only the maximum value within a certain window in the input feature map to the output feature map. We developed two different implementations for the maxpool operation which are the bandwidth heavy, and streamlined version.

**Bandwidth heavy:** the max operation within a certain window can easily be parallelized. In fact the maximum of the four values can be calculated efficiently and we can produce one output pixel in the output feature maps every clock cycle. Assuming we have sufficient bandwidth we can in fact perform the maxpool reduction to the whole input feature in one cycle however this requires reading the full feature map from memory at once which is impractical. For that, we limit the parallelization to the size of the window. In lenet, it is  $2 \times 2$  which gives us a  $4 \times$  speedup over the naive implementation of the sequential version of the problem.

**Streaming calculation:** As we aim for efficiently pipelining the operators in a convolutional neural networks. We take into consideration the fact that input feature maps will be streamed into the maxpooling layer. Therefore to perform the maxpool operation we should buffer in the whole first row and then we can proceed to produce the outputs sequentially. So assuming we are reading our data through an OpenCL channel, the way to fix this is to borrow from the already implemented solution for the sliding buffer convolution. In fact, the maxpool operation iterates over an input feature map as a convolution, however in our case, the stride size is equal to the filter dimensions  $2 \times 2$ . We adapt the sliding buffer implementation from the convolution layer to the maxpool layer and use it in our generic maxpool template.

### 3.2.3 Non-Linearities

In between convolution layers and fully connected layers, non-linear functions are applied on the output feature maps. Without non-linear functions, a neural network ( no matter how many layers it consists of ) would behave as a single layer perceptron because summing the layers would give just another linear function. We implement both classical non-linearities such as the sigmoid function and the hyperbolic tangent, in addition to the ReLU function. The ReLU non-linearity define as  $relu(x) = \max(0, x)$  has proven to increase accuracy [27], in addition to accelerating training as the derivative can be simply coded as  $relu'(x) = 1$  if  $(x \geq 0)$  else  $0$ . In terms of hardware the relu derivative is simply a MUX wired to constant values of  $0$  and  $1$ . We implement these operations as a streamlined operation which is pipelined with an  $ii$  of  $1$ .

### 3.2.4 Softmax

For the output layer we implement the *Softmax* operation. It can be used as a modular output layer for a network that performs multi-class classification such as the LeNet. The operation is defined as follows:

$$f(z_j) = \frac{e^{z_j}}{\sum_{k=1}^K e^{z_k}} \quad \text{for } j=1,\dots,K \quad (3.3)$$

and it is used to map  $K$  outputs to  $K$  possible probability values in a categorical distribution. This function highlights the maximum values and suppresses those that are a certain order of magnitude below the maximum value. Due to the interdependency for normalizing the outputs, the softmax needs to read all output values before it operates, however the operation is unrolled, and since this is the final layer, the output of this operation is written directly to memory.

### 3.2.5 Backpropagation

Backpropagation for all of the layers in the above sections. We summarize all backpropagation kernels in one section for two reasons; the first being that the backward operators borrow the same implementation from the forward calculations; i.e backpropagation of a convolutional layer is also a convolution, and backpropagation of a fully connected layer is also a matrix multiplication. We believe that the main challenge introduced by implementing backpropagation is that It requires additional buffer space to hold intermediate outputs and the gradients efficiently as soon as they are still needed. For that we are faced with two options:

- Replicate writes in the pipeline to global memory and find a way to synchronize forward and backward operations.
- Use kernels that read and write to memory and run them sequentially.

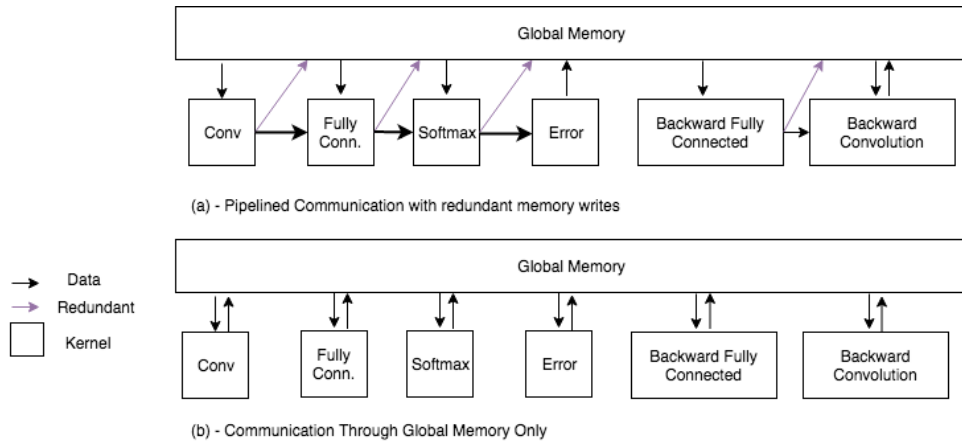


FIGURE 3.6: Two types of inter-layer communication

We choose to go with option (b) in training neural networks, though not optimal, due to time limit constraints. For inference, however, we have implemented both versions of inter-layer communication. Our backpropagation algorithm is not pipelined only due to the fact that we need to store intermediate results and this makes it easier as a first prototype for training neural networks on FPGAs. This only impacts performance slightly, because when kernels communicate through memory several parallelization techniques can be performed while sacrificing bandwidth. Since each kernel runs in a separate timeslot, the whole board bandwidth is available for the single layer which offers us more flexibility in parallelization and making use of the full bandwidth. Another thing to note is that profiling kernels is easier and we can better see the time consumed by each kernel separately and relieve bottlenecks for different operators or architectures

Backpropagation is the process of propagating an error back to the network layers in order to adjust the weights. The gradient is propagated backwards in the network based on the chain rule in differential calculus. Several weight update rules ranging from a fixed learning rate to adaptive and momentum-based methods are explored in literature [3]. In our implementation we keep the learning rate as an input argument so that it can be configured at runtime by the host program. This allows for flexibility in experimenting with different weight update rules without the need to rebuild the kernel.

The trainable weights are usually initialized to small random values in the range  $(-0.5, 0.5)$ . In practice, the random weights are then normalized depending on the weight activations used<sup>1</sup>. There are also different weight normalization schemes used in practice to mitigate ( but not completely solve ) problems that arise in deeper networks like the vanishing or exploding gradient [20]. For the ReLu activation, it is common to multiply the random weights by a factor of  $\sqrt{\frac{2}{\text{sizeof}(\text{prev.layer})}}$ . This initialization is done on the host side and the weights are then transferred to the FPGA in the beginning of the training procedure.

**Convolution Backpropagation:** The backpropagation of a convolution operator is also a convolution. For that we borrow some optimizations performed on the forward convolution such as buffering the coefficients, and unrolling over kernel dimensions. We note the main difference is that in inference phase, a window of dimensions  $K_w \times K_h$  is sliding along an input feature map in order to obtain an output feature map. Thus this is more of a *reduction* performed by multiply and accumulation of values in a specific window. In the case of propagating back an error, the input delta ( coming from the output feature map ) is *broadcast* to all of the pixels in the input feature maps ( also show a picture here ). A simple implementation would introduce memory dependencies on calculations. A different approach is to rearrange dimensions and use local buffering to hold values of the output deltas before writing to memory. The backpropagation kernel we implemented is

<sup>1</sup><https://medium.com/usf-msds/deep-learning-best-practices-1-weight-initialization-14e5c0295b94>  
Last Accessed: 25/08/2018

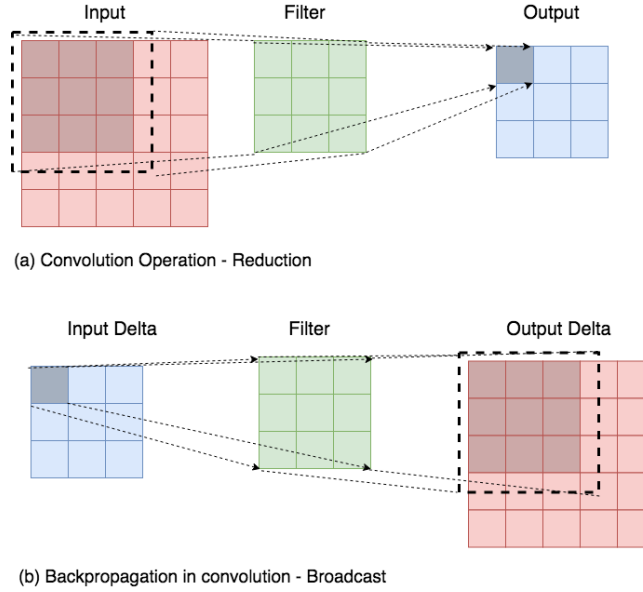


FIGURE 3.7: Propagation of data in convolution

fully pipelined with  $ii = 1$  and also performs batched weight updates for the filters.

**Maxpool backpropagation:** For backpropagation through maxpool, we simply pass upstream the error to the input pixel in a certain window with the maximum value. The same implementation from the forward max pooling is used with the addition of passing an output gradient at the maximum as opposed to passing the maximum value downstream. In our case the maxpool does not have any trainable parameter and acts as a multiplexor that passes down the error as it is.

**Fully connected backpropagation:** The fully connected layers used for classification contain most of our trainable parameters. In the case of mini-batches we use a matrix multiplication technique for both forward and backward propagation of the error. We also try to unroll computation loops to utilize the maximum bandwidth available for this kernel. The backpropagation is a similar inverse computation ( still matrix multiplication) and the weights are also updated according to a configurable learning rate.

**Loss:** For the loss function we implemented a cross entropy loss function (2.1). It measures divergence of the softmax output probabilities ( representing a categorical distribution ) with the target output probabilities given as a *one-hot* encoding.

### 3.3 OpenCL Kernel Template Generator

Many parameters such as sliding window sizes, kernel size, and number of input and output channels should be known at compile time. Each of the discussed layers is parametrized by a specific set of parameters that it takes in as a configuration. For that we created a python tool that instantiates instances given a kernel template in '.cl' format ( the extension for OpenCL kernels).

The idea is to use a configuration file in JSON to customize a specific layer. In conjunction, we used a python library called `jinja2`<sup>2</sup> to instantiate templates. Templating allows us to instantiate multiple versions of the kernel to be used and compiled together for the neural network accelerator.

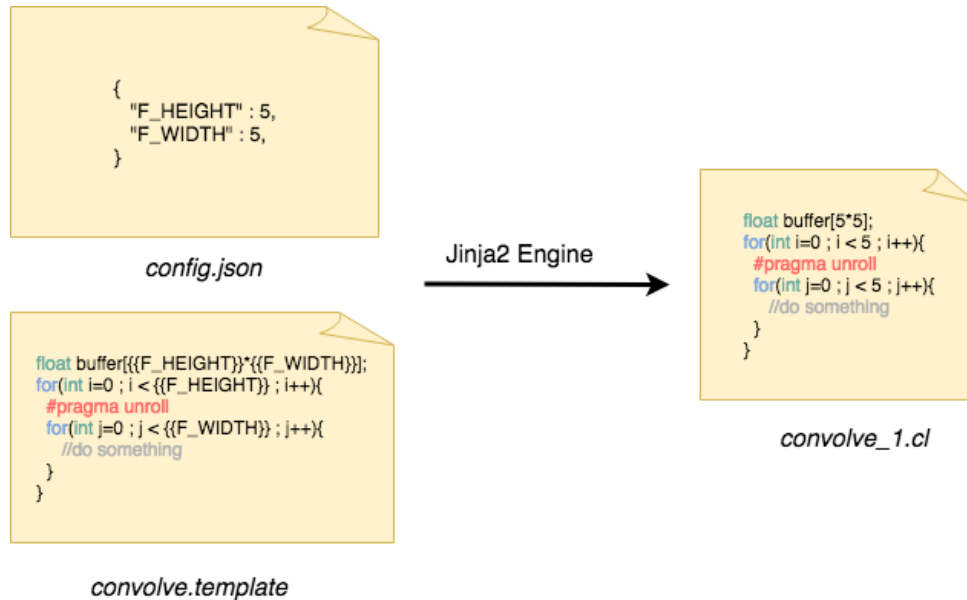


FIGURE 3.8: Templating Kernels

```

hnaous@greina2:~/dnn_fpga$ ./script.py -h
usage: script.py [-h] [-f] [-p] {cpp,emulate,report,hw} filename context

positional arguments:
  {cpp,emulate,report,hw}
                        enter a command
  filename              template file location
  context              JSON configuration file for template

optional arguments:
  -h, --help            show this help message and exit
  -f, --fast_compile    enable fast-compile
  -p, --profile          enable profiling
    
```

FIGURE 3.9: OpenCL Template Generator Usage

The basic usage is exposed through the interface shown in 3.9. The Python tool allows the user to also perform additional tasks on the generated kernel such as generating the performance report, compiling for emulation, compiling for hardware, and compiling the kernel as a C++ application using gcc. We discuss the use of compiling as a C++ application in 5.1. This type of compilation differs from the traditional workflow suggested by Intel as we have extended the emulation framework of kernels and use C++ to perform unit testing and verifying correctness of the operators. This rids us from the responsibility of creating a host program that interfaces with the kernel and

<sup>2</sup><http://jinja.pocoo.org/docs/2.10/> Last Accessed: 25/08/2018

from a lot of overhead code in managing the device buffers just for the sake of verification. As for the additional functions such as generating report, and compiling for hardware, the additional value provided by the tool is that it supports instantiating multiple templates at the same time and combining them in a single report or a single binary. All of the kernel implementations discussed in 3 are designed as templates and the generator tool is used for instantiation, and interaction with the Intel compiler to perform different types of analysis.

### 3.4 Integration with Deep500

Deep500<sup>3</sup> is a library developed internally in the Scalable and Parallel Computing Lab at ETH to aid in the process of developing custom backends for computational graphs. It enables the extension of operators, verification, network optimization, and acts as a distributed learning framework for deep neural network models. The networks are expressed in ONNX[37] format. ONNX is an open source format to represent computational graphs ( specifically deep neural networks ). It allows the interoperability between different deep learning frameworks such as torch[8] and tensorflow[1] and the exchange of models and parameters in between those frameworks for performing optimizations, training, and inference.

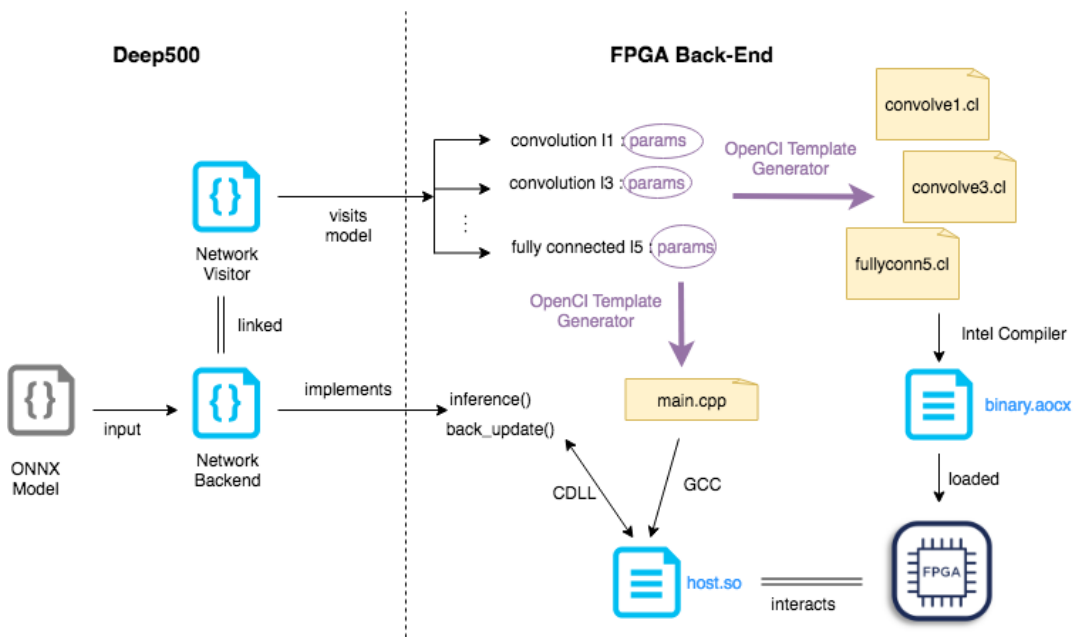


FIGURE 3.10: Custom FPGA Back-End for ONNX Models

The Deep500 library provides us with an extendable visitor interface to implement each of the operators required for a given onnx model. For example in our network, the operations we implement are convolution, max-pooling, relu, and gemm ( generalized matrix multiplication ). The Deep500

<sup>3</sup><https://github.com/deep500> Last Accessed 25/08/2018

library traverses the model's operations using a `NetworkVisitor` class. We extend the visitor class to implement all of the mentioned operations. Each visit to a node in the graph provides the parameters and input shapes required for implementing this node's operation. We use those parameters to instantiate an OpenCL kernel using the template generator we created. Then, with the `.cl` files available, we are able to transform an ONNX model into a group of inter-related OpenCL kernels that can be built for hardware 3.10. From there we can use again the tool to view the area utilization report, emulate the kernel, and perform additional unit tests on each of the operations. To enable training and inference using the kernels and built CL files, we require a host program running on the CPU that interacts with the above kernels. The host program is in C++ and has to be customized for the computational graph it runs. For that we choose to template the host program also using *jinja2*. In addition, we also use the operation parameters to be able to generate a suitable host program.

*jinja2* allows us to use nested JSON configurations and arrays in order to generate the host program. The host program performs the following operations : setting up the OpenCL environment, passing data between the host program and the FPGA's global memory buffer, and enqueueing kernels to be executed on the FPGA.

For the accelerator backend ( a python script ) to work, it should communicate with the templated host program ( C++ ), so after instantiating the host program, we compile it as a shared object '*host.so*'. This allows us to use python's CDLL library to create a handle to the C++ program. The forward and backward propagation functions are exposed externally to CDLL and we can easily pass down coefficients and inputs to the host program, which executes and returns the results.

The added value and end result of this work is given an ONNX model we can create and compile the relevant FPGA binaries by using Deep500 to traverse the graph. We are also able to instantiate and compile a controller host program, and interact with this host program to train a neural network. The benefit also extends to other popular DNN frameworks where models can be exported to ONNX. For example the `pytorch`[8] library offers the option of exporting torch models to ONNX, the implementation offers the ability to interact with this tool and train other networks on an FPGA. It is also worth mentioning that Deep500 allows us to perform unit-tests to verify each of the implemented operations on the FPGA.





## Chapter 4

# Experiments and Results

In this chapter, we describe the experiments we ran to verify the functionality of the proposed framework. We also compare different the different implementation alternatives taking kernel execution time as our main metric. All of our experiments are run on the Nallatech 510T Compute Accelerator card which contains an Alterra Arria 10 1150 GX FPGA. Our kernels are compiled with the Intel OpenCL SDK with Quartus 17.1. The host program is compiled with gcc v.7.2.0. All of the tools that support the development workflow were tested using Python 3.6.5. The model we use for training and inference is the LeNet discussed in section 3.1.

### 4.1 Convolution Implementations

#### 4.1.1 Part I : Simple Example

In this section, we compare the different convolution implementations. Those are the simple implementation, sliding buffer, and row-stationary 3.2.1. The parameters are shown in table 4.1.

The profiling results and operating frequency of the board for each of the implementations is shown in table 4.2. In the case of the row-stationary implementation, the compute array of processing elements are *autorun* kernels. Therefore they are considered to be running the whole time during execution and will not be caught by the Intel Dynamic Profiler. To approximate the time consumed we take the time difference between the reader and writer kernels that communicate with the grid as the execution time. Unsurprisingly, the row-stationary implementation is the slowest in a small example.

Parameter	Value
Image	100x100
Filter	3x3
Input/Output Channels	1

TABLE 4.1: Configuration for the Part I Test Case

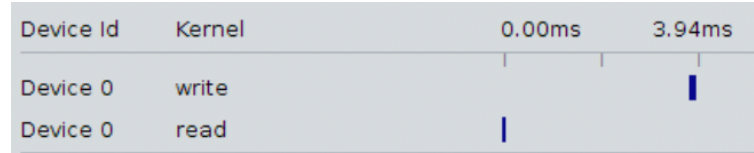


FIGURE 4.1: Dynamic Profiling result for row-stationary Implementation

Implementation	Execution Time (ms)	Frequency (MHz)
<i>Simple Implementation</i>	0.15	256.1
<i>Sliding Buffer</i>	0.09	252.8
<i>Row Stationary</i>	3.94	184.4

TABLE 4.2: Results of Part I Test

One reason is a low operating frequency due to a long critical path of execution. Another reason is the synchronization and communication overhead between the processing elements in the processing grid. We see also that the sliding buffer has the best performance in the case of a single large image which also makes sense. In the next section we abandon the row-stationary implementation and test the two other kernels in a real-case scenario.

#### 4.1.2 Part II : Performance in a Real-Case

In 4.1.1 we used a very simple two dimensional convolution to benchmark three different convolution operators. Our row-stationary implementation doesn't support a real-case convolution with multiple input and output channels. For that we compare the two other implementations ( sliding buffer, and optimized implementation 3.2.1) configured for a large batch of size of 2048 and for a convolution requiring multiple input and output channels. This allows us to better compare both operators and to choose which one is more suitable for the LeNet model.

The results are shown in table ?? . The sliding buffer is faster in practice, however it comes at the expense of more resources and a lower operating frequency. This may be feasible if we only implement the convolution operation, however in the context of a neural network, we chose the first implementation as we wish to fit more network layers in the same binary. The compiled version of the simple implementation differs from that in reference section as we have removed unrolling factors to lower the resource utilization even more. We have found that kernels with resource utilization >50% take more than 12 hours to compile and we were unable to run the full compilations without timeouts, memory limits exceeded, and placement errors.

Parameter	Value
Image	100x20
Filter	5x5
Input Channels	2
Output Channels	6
Batch Size	2048

TABLE 4.3: Configuration for Part II Test

Implementation	Total Time (s)	Frequency (MHz)	RAMS	DSP
<i>Simple Convolution</i>	5.37	232.7	85	4
<i>Sliding Buffer</i>	3.53	65.1	116	51

TABLE 4.4: Simulation Results of Different Convolution Implementations

The results are fully pipelined for the batch of images and conform to the theoretical estimate for performance. As compute time for the convolution diminishes the effect of buffering kernel coefficients, we estimate the performance taking into consideration only the main computation loop. For the simple implementation, the calculation is as follows :

Number of cycles = batch size \* input ch \* output ch \* img height \* img width \* filter height \* filter width =  $2048 * 2 * 6 * 100 * 20 * 5 * 5 = 1,228,800,000$  cycles.

The frequency of operation is 232.7 MHz, so we can estimate the time to be 5.28 seconds.

$$TotalTime = \frac{Numberofcycles}{Frequency} = \frac{1,288,800,000}{232,700,000} \approx 5.28sec \quad (4.1)$$

This theoretical calculation matches the experimental results. The same calculation can be performed to the case of the sliding buffer implementation. We note that unrolling factors in the sliding buffer reduce the number of cycles, however this is matched by a lower operating frequency as well.

## 4.2 Pipelined vs. Non-Pipelined Inference

In this example we study the effect of pipelining on the inference phase of the neural network. We test both a pipelined implementation of LeNet 3.1 where kernels are connected by Intel OpenCL Channels and the kernels follow a sliding buffer / streamlined implementation. We also test a non-pipelined version shown in 3.6, where the operators are run sequentially, communicate through global memory, and exhibit different types of parallelism. The batch size is configurable at run-time, so we test the time it takes for the inference of a single image and the time for a batch of 2048 images.

The results are that the pipelined version is effectively faster than the non-pipelined version during inference. The figure 4.2 shows the dynamic profiler results. We note that the kernels were enqueued into separate queues and also in reverse order in the host program. This is why it seems that the softmax kernel has been running the longest, but effectively it only runs after all of the layers have been completed. We noticed that running the kernels in the order that they are supposed to execute introduced latencies due to context switching and the overhead of enqueueing the tasks from the host-side, so this reverse order gives a more accurate representation of effective time taken for inference.

The kernels communicate through channels so we are sure that they are synchronized and the results are verified for correctness by using a LeNet CPU implementation configured with the same weights. The kernel also *effectively* starts running after the reader kernel starts (which is at 0.3 ms from the initial start time because it is the last to be launched and all other layers depend on its input).

The estimation is further verified by running the pipeline to classify a set of 2048 images and the total time taken in that case is 6.12 seconds. A simple calculation in 4.2 shows that the theoretical results agree with the experimental results. The dynamic profiler result in 4.3 shows that all layers are being effectively utilized in case of batch image inference.

$$\text{Total time} = \text{time for single image} * \text{batch size} = 0.03 * 2048 \approx 6.14 \text{ seconds} \quad (4.2)$$

As for the non-pipelined version, we see in 4.4 that in the case of inference for a single image, the total time taken for inference is 21.53 milliseconds. Moreover, the effective time by summing up the individual kernel execution times is much less. The reason for the delay in launching kernels is mainly synchronization constructs by calling *clFinish(queue)* in between kernel launches. Summing up individual kernel times leads to an effective execution time of 5.4 milliseconds. This is still significantly slower than the pipelined implementation. For inference of the batch, the effect of synchronization is minimized and we find that the total time of 11.15 seconds meets the theoretical results 4.3.

Implementation	Single Image (Effective)	Batch of 2048 Images
<i>Pipelined LeNet</i>	0.0033 ( 0.003 )	6.12
<i>Non-Pipelined Lenet</i>	0.021 ( 0.0054 )	11.15

TABLE 4.5: Inference time for pipelined and non-pipelined im-  
plementations of Lenet in seconds.

Batch Execution time = batch size \* effective time one image

(4.3)

= 2048 \* 0.054sec ≈ 11.05sec

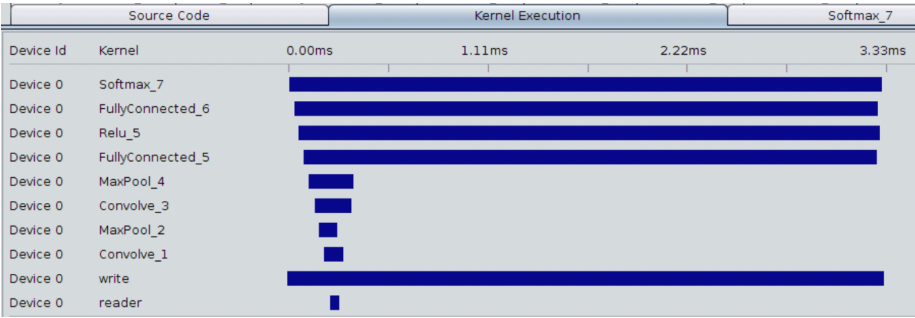


FIGURE 4.2: Execution time for inference of a single image  
(pipelined)

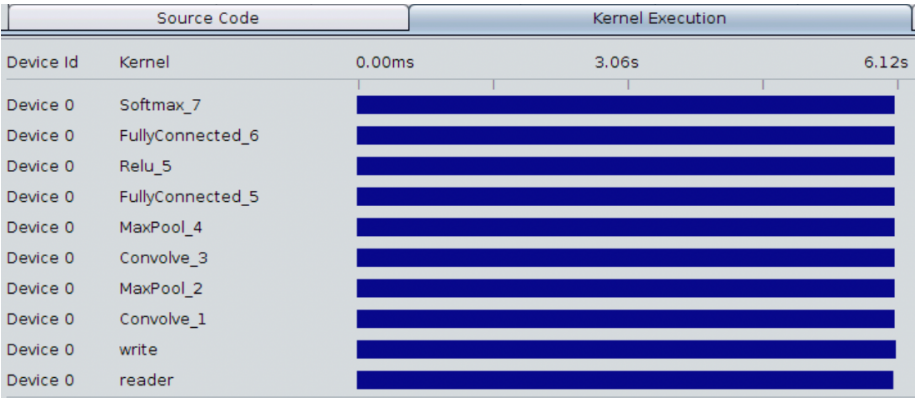


FIGURE 4.3: Execution time for inference of a batch of images  
(pipelined)

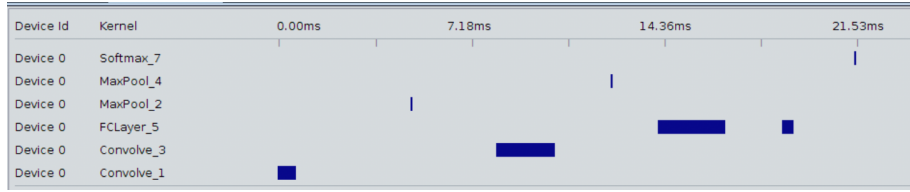


FIGURE 4.4: Execution time for inference of a single image (non-pipelined)

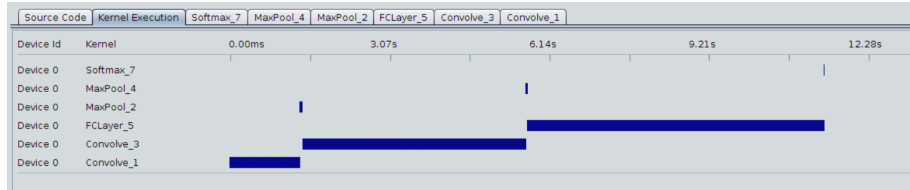


FIGURE 4.5: Execution time for inference of a batch of images (non-pipelined)

## 4.3 Training LeNet

### 4.3.1 Reconfiguration Time

We implemented full minibatch backpropagation for the LeNet model. The problem we faced is that the fully optimized kernel implementations for the forward and backward propagation do not fit in a single binary. The estimated area usage was always within the Arria 10's available resources and even less than 80% logic utilization. However, the compiler would run out of memory or crash with random error messages during compilation after tens of hours of running. For that we chose to simplify the design and break it up into a binary for forward propagation and a binary for backpropagation. The FPGA would reconfigure when switching between the two modes and in this section we evaluate the feasibility of this approach.

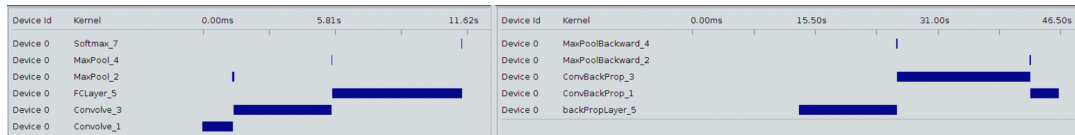


FIGURE 4.6: Dynamic Profiling results for minibatch on LeNet.

By looking at the figure 4.6 and after re-running the experiment time for multiple times, we realize that reconfiguration time is long and takes between 2 and 2.5 seconds in total. For a small batch size or in the case of a single image, reconfiguration time introduces a large overhead. When working with large batches, the effect is minimized ( as shown in table ?? ). One iteration in the table consists of kernel reconfiguration ( twice ), forward propagation, and backward propagation with weight updates for the full batch.

Batch Size	Total Epoch Time	Reconfiguration Time (x2) in seconds	$\frac{ReconfigurationTime}{TotalEpochTime}$
1	4.3	4.2	97.6 %
2048	49.1	4.6	9.3%

TABLE 4.6: write some caption here

In the case of a batch size of 2048, the overhead of reconfiguration is still large ( 9.7%), however this is more feasible to perform as opposed to a single image. Nevertheless, with larger batch sizes, we risk reaching a local minimum when optimizing the loss function as discussed before in 2.3.

### Challenges

The implementation of LeNet required a lot of modifications until we started to see a decrease in the loss function. One of the challenges was the vanishing gradient problem [20]. We solved this by replacing the ReLU function with the leaky ReLU which improved the training procedure. The Leaky ReLU function is given by 4.4.

$$f(x) = \begin{cases} x & : \text{if } x \geq 0 \\ 0.01x & : \text{otherwise} \end{cases} \quad (4.4)$$

In back-propagating the error in the fully connected layers, we experimented with gradient clipping techniques which also improved the stability in the weight updates.

We ran the batch size of 2048 on the FPGA, however it took as long as 2 hours per epoch and we did not get an improvement in accuracy. This may be due either to the batch size being too large, or because of some error introduced into the minibatch backpropagation implementation for convolutional layers. As for simply running Stochastic Gradient Descent, it is infeasible to run on the FPGA due to the overhead of reconfiguration which dominates runtime, we used the Intel Emulator and noticed a decrease in the loss function but we did not run it until convergence as the emulator crashes when too many threads are launched and destroyed.

#### 4.3.2 Simple Classifier

In this section, we compile a simple neural network composed of only fully connected layers. The number of neurons per layer is shown in table ???. We trained the model until convergence and unlike the LeNet model, both the full forward and backward propagation fit on the Arria 10 FPGA. It achieved

Layer	No. of Neurons	Trainable Parameters
<i>Input</i>	784 ( 28*28 )	0
<i>Fully Connected</i>	512	401,920
<i>Fully Connected</i>	512	262,656
<i>Fully Connected</i>	10	5130
<i>Softmax</i>	10	0

TABLE 4.7: Number of Trainable Parameters per Layer in the Simple Classifier.

reasonable runtime, 5.3 minutes per epoch and took 20 epochs to converge. We randomly sampled 5000 images of the MNIST Dataset for training and 500 images for testing. Eventually, the model achieved 67% test error. In the simple model there is a **lot** of room to tune hyperparameters. Moreover, in this experiment, we did not aim to come up with the highest accuracy or fastest runtime. The goal was to prove the correctness and the usability of the framework in which both forward and backward propagation fit on a single board configuration. Hopefully with a more advanced board, with a better fabric we can achieve better performance for more complex models.



## Chapter 5

# Intel OpenCL SDK Primer

### 5.1 Development Workflow

The standard workflow recommended by the Intel OpenCL programming guide[35] is to compile a kernel for emulation in order to verify correctness. The software emulation that Intel offers mimics the real deployment of a kernel in production and requires writing a host program to control the kernel program ( as in a typical OpenCL deployment ). This overhead of the host program includes writing code for creating and launching a kernel, allocating and managing buffer space, and a lot of overhead platform detection code which makes the overall development process slower. For that we follow a different approach to developing OpenCL kernels in order to improve functional testing for correctness during the initial stages of kernel compilation.

As OpenCL is a C-based language, kernels can be fully compiled using GCC asides from the OpenCL API specific calls. This may appear counter-intuitive as OpenCL has a different programming model, but for FPGAs we are usually writing kernels as a single Work item as opposed to NDRange kernels [46]. Knowing this, we are not explicitly using the programming model's thread parallel execution paradigm. This means that kernels can be compiled and tested as ordinary C-functions as a single work item that follows a sequential C programming style. This also makes it easier to use gdb for debugging any issues with the kernel before emulation and creating a host program.

To fully enable this feature we have abstracted the OpenCL specifics using macros as a first step. In the small example in 5.1, the *kernel* keyword informs the OpenCL compiler that this function is a kernel and not an ordinary function. We don't need this specifier when compiling for C using GCC so we specialize it only for Intel's OpenCL compiler. This is one way to allow multiple compilers to compile the same file for different objectives. Another way is to use templating engines for our files so we leave this as future work.

```

1
2 #ifdef INTELFGPA_CL  // <-- defined by the Intel OpenCL compiler
3 __kernel
4 #endif
5 void dummy() {
6     //do something;
7 }

```

LISTING 5.1: simple example of abstracting API specifics

We have automated this abstraction process and extended it to several other features like OpenCL channel communication. For that, we overrode Intel's channel API [24] functions like `read_channel_intel()` and `write_channel_intel()` and direct those to reads and writes from a thread-safe implementation of *blocking queues*. The overridden functionality is again only introduced when the kernel is compiled with GCC and not the Intel compiler. When testing with multiple kernels, each kernel is launched in a separate thread and we can successfully emulate a multi-threaded environment and can debug errors in communication between the kernels such as queue starvation or overflow. Template files would be another option for abstracting those specifics, so we leave this as future work for now. This development workflow serves as a first step to writing generic C-functions with cross-platform support.

## 5.2 Single Work-item vs ND-Range Kernel

OpenCL's view of shared memory fits more closely to GPUs than FPGAs, the need for portability of code for different architectures is still an ultimate goal that would enable efficient acceleration across different hardware devices. This is mainly why we see FPGA manufacturers like Altera and Xilinx improving the SDKs for supporting the development of FPGA kernels using OpenCL. Usually by using OpenCL's programming model [46], parallelism can be achieved by exploiting the ND-range kernel feature to parallelize a lot of work. Parallelization is done when the work is split up into multiple work groups consisting of work items. This division can be represented along one, two, or even three dimensions. This parallelization is useful and makes coding easier as the inputs and intermediate feature maps in the case of a convolutional neural networks are multidimensional and can easily be split. This splitting allows the GPU to execute these kernels simultaneously on separate processors.

In terms of supporting this, an FPGA has a fixed architecture and cannot invoke copies of the same kernel dynamically through a host program. Moreover, the specification by Intel recommends the use of single work-items when there are memory dependencies between the different work items. Synchronization in an NDRange programming model will thus result in pipeline flushes thus decreasing the pipeline efficiency. For that full efficiency can be better achieved by using the single-work item model. For example shift registers can only be inferred only in the single-work item as we need to have a main loop that accepts input and performs the shift operation at every iteration. For that, we use only single work-item kernels in our work as this allows us to perform multiple optimizations that are only possible at compile time and not host-program runtime.

In case, thread level parallelism is required, and there are no interdependencies, this can be done by wrapping the function in a loop and unrolling over the computation which provides a more efficient implementation in hardware.

## 5.3 Inferring Shift-Registers

We discussed before how one of the convolution implementations 3.1 relies on a shift-register for storing a sliding window of the input feature map. The trick to make that work is to create a loop that does the shift operation and ( move all items by one position ) and then explicitly specify the *unroll* pragma so that the compiler can perform this optimization. An example is shown in listing 5.3.

```

1 __kernel
2 void example() {
3     ...
4
5     int shift_reg[SIZE]; // SIZE is a compile time constant
6
7     while(not_finished){
8
9         #pragma unroll    // <- must specify this
10        for(int j =0 ; j < SIZE-1 ; j++){
11            shift_reg[i] = shift_reg[i+1];
12        }
13        shift_reg[SIZE-1] = read_channel_intel(in);
14
15        //do something
16
17    } //end while
18
19    ...
20 }
```

LISTING 5.2: Shift Register Inference

## 5.4 Reconfiguring the FPGA

Some tasks may require reprogramming an FPGA during runtime. The Intel FPGA specifies very little about reprogramming a kernel during host runtime. Since reprogramming takes a considerably large time ( $\approx 2 - 2.5\text{sec}$ ), it doesn't make sense to trigger this feature often. We have used this feature in training a neural network with large batch sizes to minimize the delay introduced by reconfiguration. In the training experiment we compiled the forward and backward propagation kernels into two separate binaries as they were too large to be synthesized together in the same design. It is suitable only when batching with large sizes such as 2048 so that reprogramming time is minimal with respect to actual compute time.

Our advice for this to work is that one must make sure to finish running kernels by running *clFinish(queue)* on all of the task queues and cleanup resources in a separate *cleanup()* procedure when switching between configurations. The cleanup procedure should clear all buffers used by the kernels, then the kernels themselves. The program binary then has to be recreated with the second kernel through a call to *createProgramFromBinary()*. Under the hood, this function creates a handle to the device and reprograms

it given the binary string of the new kernel we wish to use. Also it is not guaranteed that when re-allocating buffers in global memory that they will contain the same old values, therefore one must make sure to transfer everything in global memory back and forth between the device and the host when reconfiguring separate kernels.

## 5.5 Loops

The general advice for loops is that the less loops the better. When working with multidimensional grids it is natural to use multiple nested loops, however this decreases the efficiency of the static code optimizer. We introduce a workaround for collapsing nested loops into a single loop. This optimization was also discussed by [56]. For example a nested loop 5.5 can be collapsed to onw loop as in 5.5.

```

1 for(int y=0; y < m; y++){
2   for(int x=0; x < n; x++){
3     compute(y, x);
4   }
5 }

```

LISTING 5.3: nested loops, src[56]

```

1 int x = 0, y = 0;
2 while (y != m) {
3   compute (x,y);
4   x++;
5   if (x == n) {
6     x = 0;
7     y ++;
8   } //end if
9 } //end while

```

LISTING 5.4: collapsed loops, src[56]

This allows the optimizer to better resolve the loop exit conditions and enable it to resolve the condition in one clock cycle. Also the nested structures require additional hardware to preserve state in between iterations. It is also better practice to limit variables to the scope of variables to only where they are used and not in higher level loops and collapsing loops can be a measure against this.

## 5.6 Loop-Carried Memory Dependencies

When using OpenCl, it is easy forget that we are not developing a CPU application, so we tend discard unnecessary data structures and we do not consider memory dependencies in between instructions. When programming an FPGA however, it is important to relieve memory dependencies within iterations in order to get an optimal pipelined structure scheduled with an iteration interval  $ii = 1$ . Memory dependencies introduce stalls into the dataflow must wait until the result of a previous iteration is ready before proceeding to the next instruction.

For that we can use local memory to relieve dependencies and hold intermediate results, after that reductions can be performed on this local storage and the overall pipeline would become more efficient on the expense of a

higher resource usage. A simple example in Intel’s Best Practices Guide [25] shows how one can use a register to hold intermediate results and relieve the loop-carried dependencies. We extend Intel’s example when the requirement is to have a mix of pipelining and unrolling of an inner loop. Unrolling in an inner loop increases the critical path for the loop carried dependencies.

To overcome this problem, our solution consists of combining two optimizations. The first step is to transfer the dependency from global memory to a local register. The second step is to compile with the *-fp-relaxed* compiler option so that the reduction on the local register is relaxed and performed in a tree-style adder without dependencies 5.6.

```

1 #define N 200
2 #define X 10
3
4 __kernel
5 void bad_example(__global float* restrict in,
6                 __global float* restrict out){
7
8     for(int i =0; i < N; i++){
9         #pragma unroll
10        for(int j =0 ; j < X ; j++){
11            out[i] += in[i*X + j]; // memory dependency
12        }
13    }

```

LISTING 5.5: Loop-carried dependencies

```

1 #define N 200
2 #define X 10
3
4 __kernel
5 void good_example(__global float* restrict in,
6                  __global float* restrict out){
7
8     for(int i =0; i < N; i++){
9         float temp=0.0;
10
11        #pragma unroll
12        for(int j =0 ; j < X ; j++){
13            temp += in[i*X + j]; // mem <- register
14        }
15
16        out[i] = temp; // register <- mem
17    }

```

LISTING 5.6: Dependencies are transferred to a local register

In some cases, we do not wish to use the *-fp-relaxed* because we care about the numerical stability in other places in the code. In that case the memory dependency can be transferred to a local array of registers, and a reduction can be transferred on that array 5.6. This is effectively implementing the *-fp-relaxed* option on part of the code. We use this solution in our convolution operation as we also perform additional processing on the intermediate array of registers.

```

1 #define N 200
2 #define X 10
3
4 __kernel
5 void good_example(__global float* restrict in,
6                  __global float* restrict out){
7
8     for(int i =0; i < N; i++){
9
10
11         float temp[X];
12         float temp_sum = 0.0
13
14         #pragma unroll
15         for(int j =0 ; j < X ; j++){
16             temp[j] = in[i*X + j];           // mem ← local array
17         }
18
19         #pragma unroll
20         for(int j =0 ; j < X ; j++){
21             temp_sum += temp[j]; // local array ← register
22         }
23
24         out[i] = temp_sum; // register ← mem
25     }

```

LISTING 5.7: Dependency transferred to a local array

## 5.7 Using Multiple Queues

In order to execute multiple kernels concurrently, one must instantiate multiple command queues and enqueue the concurrent tasks separately within the same program. This is especially important for concurrent kernels that communicate through channels [24]. Multiple queues should be considered in the emulation stage as well, since the emulator processes tasks sequentially, unless there are multiple queues involved, then it launches multiple threads to consume from the different queues at the same time.

## Chapter 6

# Conclusion

The hype over deep learning shows no signs of slowing down. With access to larger datasets, researchers are experimenting with different architecture and the trends are generally towards deeper networks with an increasing number of parameters [3]. Training times become longer with such complex models. This makes it increasingly important to leverage hardware accelerators that benefit from the inherent parallelism in the training process of neural networks [3]. FPGAs offer a lot of advantages as opposed to other hardware accelerators as they introduce a large design exploration space.

In this work, we made use of Intel's OpenCL SDK [24] to build a modular framework for training deep neural networks. We discussed our custom development workflow to make development using OpenCL faster and more efficient and also highlighted the challenges faced. We also built the main operators that are the basic blocks for modern convolutional neural networks on and simulated it on an the Altera Arria 10 GX FPGA. By using the Deep500 library, we were also able to extend the benefits of this framework to support Open Source ONNX models. Deep500 also allowed us to build a hardware implementation that performs both inference and backpropagation. We have also benchmarked different implementations of the convolution operators and discussed trade-offs. We have also performed integration testing and proof of correctness of the implementation.

The framework is still a long way from being done and a lot of work can be done to extend it. For now it serves as a proof of concept, provides the right toolset, and lays the foundation for more optimizations and a wider range of supported layers types and operators. In practice, we have seen modern implementations with lower precision have proven to work well on FPGAs with little sacrifice on the accuracy of models [18]. This remains as future work to be experimented with. It is challenging to port lower precision to OpenCL as fixed point types are not currently supported by the OpenCL language, however, they can still be implemented by using integer operations and bit-masking techniques.





# Bibliography

- [1] Martín Abadi et al. “Tensorflow: a system for large-scale machine learning.” In: *OSDI*. Vol. 16. 2016, pp. 265–283.
- [2] Martín Abadi et al. “Tensorflow: a system for large-scale machine learning.” In: *OSDI*. Vol. 16. 2016, pp. 265–283.
- [3] Tal Ben-Nun and Torsten Hoefler. “Demystifying Parallel and Distributed Deep Learning: An In-Depth Concurrency Analysis”. In: *arXiv preprint arXiv:1802.09941* (2018).
- [4] James Bergstra et al. “Theano: Deep learning on gpus with python”. In: *NIPS 2011, BigLearning Workshop, Granada, Spain*. Vol. 3. Citeseer. 2011, pp. 1–48.
- [5] Sheng Chen, Colin FN Cowan, and Peter M Grant. “Orthogonal least squares learning algorithm for radial basis function networks”. In: *IEEE Transactions on neural networks* 2.2 (1991), pp. 302–309.
- [6] Yu-Hsin Chen et al. “Eyeriss: An energy-efficient reconfigurable accelerator for deep convolutional neural networks”. In: *IEEE Journal of Solid-State Circuits* 52.1 (2017), pp. 127–138.
- [7] Sharan Chetlur et al. “cuDNN: Efficient Primitives for Deep Learning”. In: *CoRR* abs/1410.0759 (2014). arXiv: [1410.0759](https://arxiv.org/abs/1410.0759). URL: <http://arxiv.org/abs/1410.0759>.
- [8] Ronan Collobert, Samy Bengio, and Johnny Marithoz. *Torch: A Modular Machine Learning Software Library*. 2002.
- [9] Ronan Collobert, Koray Kavukcuoglu, and Clément Farabet. “Torch7: A matlab-like environment for machine learning”. In: *BigLearn, NIPS workshop*. EPFL-CONF-192376. 2011.
- [10] Katherine Compton and Scott Hauck. “Reconfigurable computing: a survey of systems and software”. In: *ACM Computing Surveys (csuR)* 34.2 (2002), pp. 171–210.
- [11] Jason Cong and Bingjun Xiao. “Minimizing computation in convolutional neural networks”. In: *International conference on artificial neural networks*. Springer. 2014, pp. 281–290.
- [12] Balázs Csanád Csáji. “Approximation with artificial neural networks”. In: *Faculty of Sciences, Eötvös Loránd University, Hungary* 24 (2001), p. 48.
- [13] C Cuda. *Programming guide*. 2012.
- [14] Jeffrey Dean et al. “Large scale distributed deep networks”. In: *Advances in neural information processing systems*. 2012, pp. 1223–1231.

- [15] Roberto DiCecco et al. "Caffeinated FPGAs: FPGA framework for convolutional neural networks". In: *Field-Programmable Technology (FPT), 2016 International Conference on*. IEEE. 2016, pp. 265–268.
- [16] Carlos M Fonseca and Peter J Fleming. "An overview of evolutionary algorithms in multiobjective optimization". In: *Evolutionary computation* 3.1 (1995), pp. 1–16.
- [17] Rajesh Gupta and Forrest Brewer. "High-Level Synthesis: A Retrospective". In: *High-Level Synthesis: From Algorithm to Digital Circuit*. Ed. by Philippe Coussy and Adam Morawiec. Dordrecht: Springer Netherlands, 2008, pp. 13–28. ISBN: 978-1-4020-8588-8. DOI: [10.1007/978-1-4020-8588-8\\_2](https://doi.org/10.1007/978-1-4020-8588-8_2). URL: [https://doi.org/10.1007/978-1-4020-8588-8\\_2](https://doi.org/10.1007/978-1-4020-8588-8_2).
- [18] Suyog Gupta et al. "Deep learning with limited numerical precision". In: *International Conference on Machine Learning*. 2015, pp. 1737–1746.
- [19] Kaiming He et al. "Deep residual learning for image recognition". In: *Proceedings of the IEEE conference on computer vision and pattern recognition*. 2016, pp. 770–778.
- [20] Sepp Hochreiter. "The vanishing gradient problem during learning recurrent neural nets and problem solutions". In: *International Journal of Uncertainty, Fuzziness and Knowledge-Based Systems* 6.02 (1998), pp. 107–116.
- [21] Itay Hubara et al. "Binarized neural networks". In: *Advances in neural information processing systems*. 2016, pp. 4107–4115.
- [22] David H Hubel and Torsten N Wiesel. "Receptive fields, binocular interaction and functional architecture in the cat's visual cortex". In: *The Journal of physiology* 160.1 (1962), pp. 106–154.
- [23] Forrest Iandola et al. "Densenet: Implementing efficient convnet descriptor pyramids". In: *arXiv preprint arXiv:1404.1869* (2014).
- [24] FPGA Intel. "SDK for OpenCL". In: *Programming Guide*. UG-OCL002 31 (2016).
- [25] FPGA Intel. *SDK for OpenCL, Best practices guide* (2017).
- [26] Yangqing Jia et al. "Caffe: Convolutional architecture for fast feature embedding". In: *Proceedings of the 22nd ACM international conference on Multimedia*. ACM. 2014, pp. 675–678.
- [27] Alex Krizhevsky, Ilya Sutskever, and Geoffrey E Hinton. "Imagenet classification with deep convolutional neural networks". In: *Advances in neural information processing systems*. 2012, pp. 1097–1105.
- [28] Griffin Lacey, Graham W Taylor, and Shawki Areibi. "Deep learning on fpgas: Past, present, and future". In: *arXiv preprint arXiv:1602.04283* (2016).
- [29] Andrew Lavin and Scott Gray. "Fast algorithms for convolutional neural networks". In: *Proceedings of the IEEE Conference on Computer Vision and Pattern Recognition*. 2016, pp. 4013–4021.

- [30] Yann LeCun, Yoshua Bengio, and Geoffrey Hinton. "Deep learning". In: *nature* 521.7553 (2015), p. 436.
- [31] Yann LeCun et al. "Gradient-based learning applied to document recognition". In: *Proceedings of the IEEE* 86.11 (1998), pp. 2278–2324.
- [32] Grant Martin and Gary Smith. "High-level synthesis: Past, present, and future". In: *IEEE Design & Test of Computers* 26.4 (2009), pp. 18–25.
- [33] John McCarthy et al. "A proposal for the dartmouth summer research project on artificial intelligence, august 31, 1955". In: *AI magazine* 27.4 (2006), p. 12.
- [34] UA Muller and A Gunzinger. "Neural net simulation on parallel computers". In: *Neural Networks, 1994. IEEE World Congress on Computational Intelligence., 1994 IEEE International Conference on*. Vol. 6. IEEE. 1994, pp. 3961–3966.
- [35] Aaftab Munshi et al. *OpenCL programming guide*. Pearson Education, 2011.
- [36] Eriko Nurvitadhi et al. "Can fpgas beat gpus in accelerating next-generation deep neural networks?" In: *Proceedings of the 2017 ACM/SIGDA International Symposium on Field-Programmable Gate Arrays*. ACM. 2017, pp. 5–14.
- [37] ONNX. <https://github.com/onnx/onnx>. Accessed: 2018-08-22.
- [38] Yohhan Pao. "Adaptive pattern recognition and neural networks". In: (1989).
- [39] Rajat Raina, Anand Madhavan, and Andrew Y Ng. "Large-scale deep unsupervised learning using graphics processors". In: *Proceedings of the 26th annual international conference on machine learning*. ACM. 2009, pp. 873–880.
- [40] Frank Rosenblatt. *The Perceptron : a theory of statistical separability in cognitive systems*. eng. United States Department of Commerce, 1958.
- [41] Sebastian Ruder. "An overview of gradient descent optimization algorithms". In: *arXiv preprint arXiv:1609.04747* (2016).
- [42] David E Rumelhart, Geoffrey E Hinton, and Ronald J Williams. "Learning representations by back-propagating errors". In: *nature* 323.6088 (1986), p. 533.
- [43] Suhap Sahin, Yasar Becerikli, and Suleyman Yazici. "Neural network implementation in hardware using FPGAs". In: *International Conference on Neural Information Processing*. Springer. 2006, pp. 1105–1112.
- [44] Karen Simonyan and Andrew Zisserman. "Very deep convolutional networks for large-scale image recognition". In: *arXiv preprint arXiv:1409.1556* (2014).
- [45] Nitish Srivastava et al. "Dropout: a simple way to prevent neural networks from overfitting". In: *The Journal of Machine Learning Research* 15.1 (2014), pp. 1929–1958.

- [46] John E Stone, David Gohara, and Guochun Shi. "OpenCL: A parallel programming standard for heterogeneous computing systems". In: *Computing in science & engineering* 12.3 (2010), pp. 66–73.
- [47] Vivienne Sze et al. "Efficient processing of deep neural networks: A tutorial and survey". In: *Proceedings of the IEEE* 105.12 (2017), pp. 2295–2329.
- [48] Christian Szegedy et al. "Going deeper with convolutions". In: *Proceedings of the IEEE conference on computer vision and pattern recognition*. 2015, pp. 1–9.
- [49] Nicolas Vasilache et al. "Fast convolutional nets with fbfft: A GPU performance evaluation". In: *arXiv preprint arXiv:1412.7580* (2014).
- [50] Dong Wang, Ke Xu, and Diankun Jiang. "PipeCNN: an OpenCL-based open-source FPGA accelerator for convolution neural networks". In: *Field Programmable Technology (ICFPT), 2017 International Conference on*. IEEE. 2017, pp. 279–282.
- [51] Kaining Wang and Anthony N Michel. "Robustness and perturbation analysis of a class of artificial neural networks". In: *Neural networks* 7.2 (1994), pp. 251–259.
- [52] Bernard Widrow and Michael A Lehr. "30 years of adaptive neural networks: perceptron, madaline, and backpropagation". In: *Proceedings of the IEEE* 78.9 (1990), pp. 1415–1442.
- [53] Peter Wilson. *Design Recipes for FPGAs: Using Verilog and VHDL*. Newnes, 2015.
- [54] AXI Xilinx Vivado. *Reference Guide*.
- [55] Chen Zhang et al. "Optimizing FPGA-based Accelerator Design for Deep Convolutional Neural Networks". In: *Proceedings of the 2015 ACM/SIGDA International Symposium on Field-Programmable Gate Arrays*. FPGA '15. Monterey, California, USA: ACM, 2015, pp. 161–170. ISBN: 978-1-4503-3315-3. DOI: [10.1145/2684746.2689060](https://doi.org/10.1145/2684746.2689060). URL: <http://doi.acm.org/10.1145/2684746.2689060>.
- [56] Hamid Reza Zohouri, Artur Podobas, and Satoshi Matsuoka. "Combined spatial and temporal blocking for high-performance stencil computation on FPGAs using OpenCL". In: *Proceedings of the 2018 ACM/SIGDA International Symposium on Field-Programmable Gate Arrays*. ACM. 2018, pp. 153–162.